Dipartimento di Biologia

Corso in Biologia applicata alla Biomedicina

CLONING TRPC1 TO ENHANCE CALCIUM SIGNAL IN A MODEL OF BITTER TASTE TRANSDUCTION

CANDIDATA

Noemi Barsotti

RELATORI

Prof. Dal Monte Massimo

Dr. Alessandro Marchiori

Anno Accademico 2013/2014

INDEX

1. INTRODUCTION

The sense of taste allows animals to detect food-derived chemicals, guiding to identify and consume nutrients, while avoiding toxins and harmful substances.
Mammalian, and so humans, can detect and distinguish between, at least, five basic taste qualities: sweet, bitter, umami, sour and salty (Breslin et al., 2008) [Fig.1]. Each one is referred to nutritional and physiological requirements or to potential hazards:

- Sweet taste signals the presence of carbohydrates used as energy by organism. This taste has been proposed to activate the reward circuit in the brain and thus to induce feeding behavior.
- Salty taste governs intake of Sodium and other salts, to maintain blood circulation and body's water balance.
- Umami is thought to be important to detect L-glutamate and other L-amino acids, representing food's protein content.
- Sour and bitter tastes are important to perceive potentially noxious substances. Sour taste signals the presence of acids and generally is aversive, preventing from ingesting excess of acids or acid substances produced during spoilage of food.
- Bitter taste is naturally aversive and is thought to be protective against ingestion of toxins, many of which are of genuine plant origin or produced during aging, spoilage or processing of food, like fermentation reactions. Therefore the ability to detect bitter substances and the onset of aversive response to these foods is thought to be an evolutionary advantage.

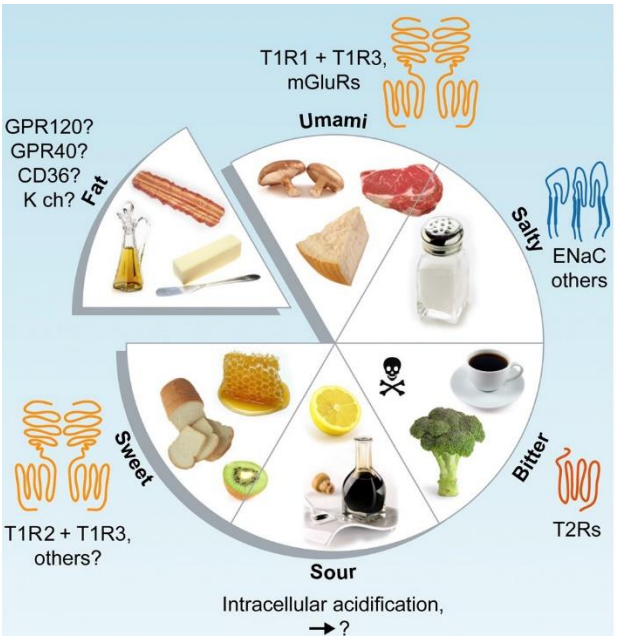

Figure 1: Taste qualities and receptors that detect them. Bitter taste is thought to protect against ingestion of harmful substances and is transduced by G protein-coupled receptors, as well as sweet and umami tastes. Sweet taste detects sugars and carbohydrates. Umami taste signals L-amino acid and nucleotides. Na^+ is detected by salty taste. Sour taste is another defender of organism sensing organic acids (from Chaudari & Roper 2010).

1.1 Taste morphology

Humans taste with the edge and the dorsal of the tongue, soft palate and pharynx. (Breslin et al., 2006). These tissues comprise gustatory epithelia which contains taste buds, the sensory organs. A taste bud is a cluster of 60-70 up to 100 polarized cells, embedded in the stratified epithelium and shielded from the environment by means of tight junctions in basolateral region (Michling et al., 2007*)* [Fig.2]. On the tongue, taste buds are within small bumps or folds, called papillae. We can find fungiform papillae on the anterior tongue, circumvallate papillae on the posterior tongue and taste buds buried in folds on lateral sides of the tongue, in foliate papillae [Fig.3].

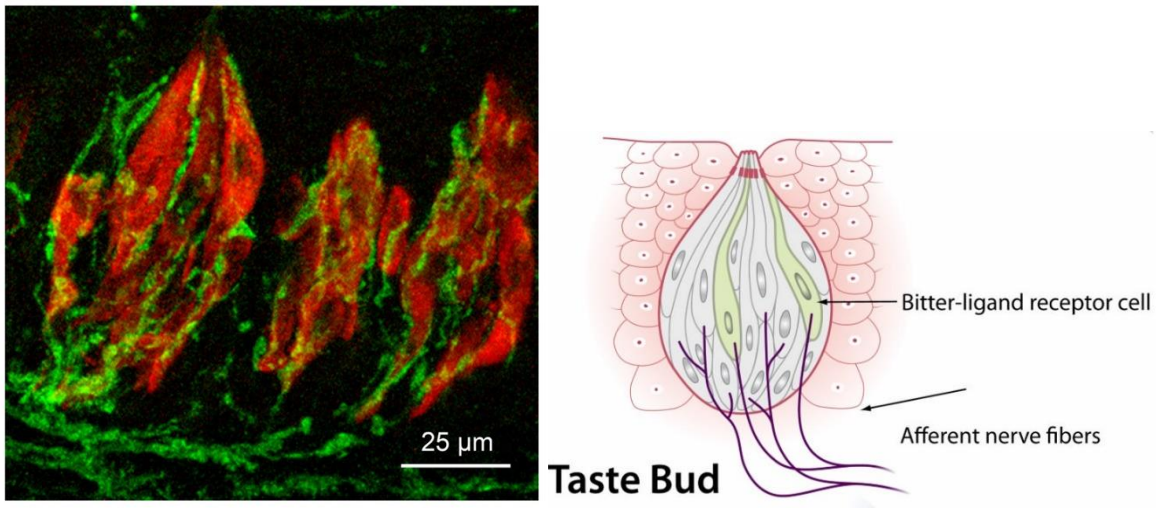

Figure 2: On the left, micrograph of three taste buds in the circumvallate papilla of a mouse. It is possible to note Type II taste cells stained red and gustatory afferent fibers stained green. In this longitudinal section surface of the epithelium is at the top of the micrograph (from Kinnamon & Finger, 2013). On the right, scheme of taste bud with afferent nerve fibers reaching TCRs and Type III cells (adapted from Mennella et al., 2013).

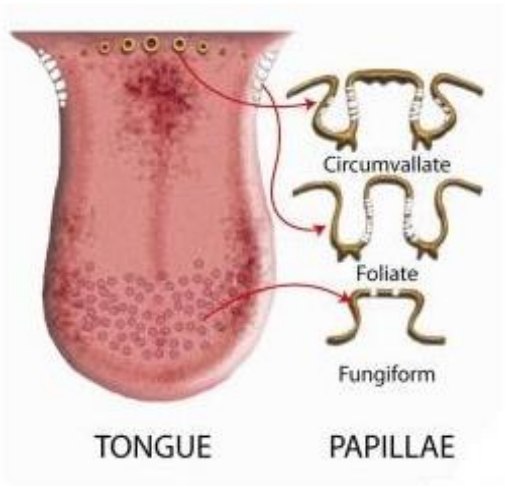

Figure 3 : Human papillae on tongue. Taste buds cluster in three types of papillae. The simplest are fungiform papillae located on the tip of tongue. Circumvallate and foliate papillae are more complex and are located on the posterior tongue, near the root, and on the sides of the tongue, respectively (from Martin et al., 2009).

Every taste bud is a community of interacting cells falling into three major categories, defined by their morphological appearances (Murray, 1993; Pumplin et al., 1997; Yee et al., 2001), by proteins expression (Yang et al., 2000; Yee et al., 2001; Clapp et al., 2004) and by their gustatory responses.

Type I cells are believed to have glial-like functions (Dvoryanchikov et al., 2009) as synthesize and deposit ecto-ATPase on their surface that degrades the transmitter released by other taste cells (Bartel et al., 2006). Even more they express GLAST, a transporter of glutamate, thus Type 1 cells appear to be involved in terminating synaptic transmission. In the end Type 1 cells may exhibit ionic currents involved in salt taste transduction (Vandenbeuch et al., 2008).

Type II cells are called also Taste Receptor Cells (TRCs) (DeFazio et al., 2006), expressing G protein-coupled receptors (GPCRs) for sweet, umami and bitter taste compounds. Moreover these cells express the downstream proteins of GPCRs taste signal pathway as PLCβ2 (Chaudari & Roper, 2010). Every TRC is tuned only to one specific taste stimuli but bitter responsive taste cells can express subsets of TAS2Rs with partially overlapping receptive ranges (Chandrashekar et al., 2006; Yarmolinsky & Zuker, 2009, Behrens et al., 2007).

TRCs are electrically excitable cells, due to the expression of voltage-gated Na^+ and K^+ channels essential for evoking action potentials (Chen et al., 1996) and secreting ATP as neurotransmitter (Finger et al., 2005). The release of ATP likely happens through Pannexin-1 hemichannels (Dando & Roper, 2009; Romanov et al., 2012). It is interesting to note that Type 2 cells do not form identifiable synapses, but nerve fibers are found in close proximity to these cells (Murray et al., 1993; Yang et al., 2000; Yee et al., 2001; Clapp et al., 2004).

Type III cells are also called “presynaptic” (DeFazio et al., 2006) because they form synaptic junctions with nerve terminals and express proteins associated with synapses or neuronal cells, like SNAP25 and NCAM (Clapp et al., 2004; DeFazio et al., 2006). Even more they show depolarization-dependent Ca^{2+} transients typical of synapses (DeFazio et al., 2006). Like receptor cells, presynaptic cells express voltage-gated Na^+ and K^+ channels to support action potentials (Vandenbeuch & Kinnamon, 2009). Type III cells also respond directly to sour stimuli and are responsible of this taste quality, likely involving apically located ion

channels. The sour stimuli leads to secretion of neurotransmitters serotonin and GABA (Huang et al., 2011).

A very important role of presynaptic cells seems to be receiving input and integrating signals coming from TRCs. Thus, Type III cells are not tuned to specific taste qualities, but rather respond to every detected compound (Tomchik et al., 2007).

Another type of cells found in taste buds is basal cells, the so-called *Type IV*, that comprises spherical and ovoid cells that are likely undifferentiated or immature taste cells (Farbman, 1965).

1.2 Signal transduction

Only at the pore of taste bud the apical region of the cells is directly in contact with the external environment, sensing taste stimuli present in the oral cavity. Like stated above, presynaptic cells detect sour taste stimuli. Even though the specific transduction channels or receptors remain elusive, seems that the permeation of protonated acid (RCOOH) across plasma membrane and the consequently dissociation in anion ($RCOO^-$) and proton (H^+) leads to cytosolic acidification and this allows cation influx and then membrane depolarization (Lyall et al., 2001; Huang et al., 2008). Type III cells express voltage-gated Ca^{2+} channels, so the depolarization allows Ca^{2+} influx that determines vesicular secretion of serotonin, GABA (Huang et al., 2011), and probably norepinephrine (Huang et al., 2008).

Cells and receptors responsible of salt taste detection are still unknown. It has been proposed that Epithelial Na^+ Channels (ENaC) guide salt transduction in rodents (Heck et al., 1984; Chandrashekar et al., 2010) and that Type I cells express ENaC (Vandenbeuch et al., 2008). This would lead to the conclusion that type I cells are responsible for Na^+ taste, but there are not yet definitive evidences.

Type II cells express GPCRs to sense sweet, bitter and umami tastes. In the last two decades two families of these receptors have been identified, renamed TAS1R and TAS2R for sweet and bitter compounds, respectively. Cells expressing the heterodimer TAS1R2+TAS1R3 detect sugars, synthetic sweeteners and sweet-tasting proteins (Nelson et al., 2001; Jiang et al., 2004; Xu

et al., 2004). Although mice lacking TAS1R3 conserve sweet perception (Damak et al., 2003), suggesting the existence of additional sweet receptor, candidate has not yet been proposed.

Umami taste is sensed by heterodimer TAS1R1+TAS1R3 which responds particularly to the combination of L-glutamate and GMP/IMP, found in food after hydrolysis of proteins and nucleotides (Li et al., 2002; Nelson et al., 2002).

Being GPCRs, TAS1Rs and TAS2Rs are seven helices transmembrane receptors, but while TAS1Rs are dimeric Class III GPCRs, with a large N-terminal extracellular domain (Max et al., 2001) and more binding sites, TAS2Rs belong to Class I GPCRs with a short N-terminal domain, with ligand binding region in the extracellular loop and transmembrane domains, similar to the opsins and the olfactory receptors (Adler et al., 2000; Chandrashekar et al., 2000) [Fig.4]. Relatively recent data suggest that intracellular carboxy terminal regions are particularly important for agonist selectivity (Brockhoff et al., 2010). In this study swapping amino acids in transmembrane segment 7 was used to invert agonist selectivity. TAS2R43, TAS2R44 and TAS2R46 were used and the result was indeed the reversal of specificity. This suggested that TAS2Rs have a single binding pocket overlapping a set of amino acids to accommodate different agonists, while the contribution of extracellular loop regions seems to be less important.

Both cytoplasmic part of transmembrane domain and intracellular loops are well conserved, while extracellular part are much less. Another well-conserved region lies in second extracellular domain where N-glycosylation sites are present. Since TAS2Rs are transmembrane receptors an effective signal targeting is fundamental. Indeed TAS2Rs missing N-glycosylation have low membrane expression (Reichling et al., 2008).

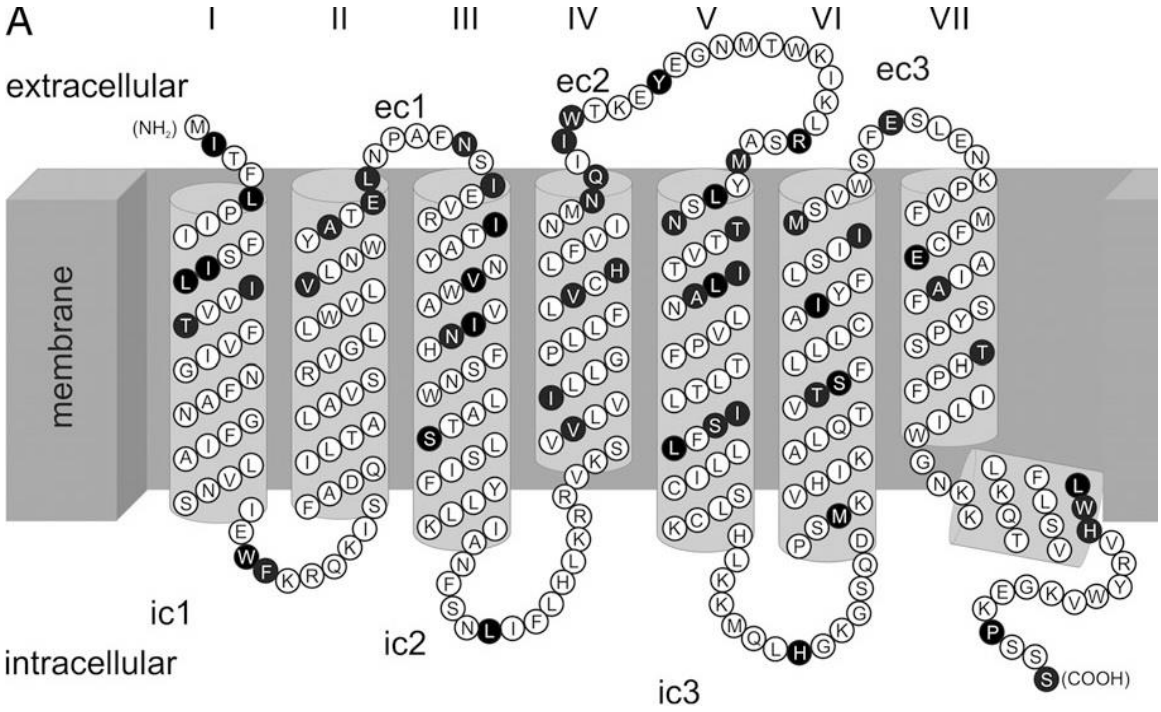

Figure 4 : hTAS2R46 snake plot. Roman numbers indicate transmembrane domains. Extracellular loops are indicated as ec, intracellular loops as ic (from Brockhoff et al., 2010).

When bitter tastant binds to one or more bitter taste receptor, subsequent conformational change leads to activation of a taste-specific G protein, α-gustducin (McLaughlin et al., 1992) and it's βγ partners, β3 or β1 and γ13 (Huang et al., 1999). The principal pathway of bitter taste transduction appears to be via Gβγ, receptor conformational change causes Gα and βγ subunits to split from each other, thus allowing βγ subunit to activate a specific phospholipase PLCβ2, an unusual isoform activated by Gβγ rather than $G\alpha_q$ family subunits (Rössler et al., 1998). PLCβ2 converts the membrane lipid PIP_2 into the second messengers 1, 4, 5-inositol trisphosphate (IP_3) and diacylglycerol (DAG). While the role of DAG is still unclear, IP_3 binds to the Type III IP_3 receptor (IP_3R) on the membranes of endoplasmic reticulum (ER) leading to Ca^{2+} release from the intracellular stores (Clapp et al., 2001; Miyoshi et al., 2001). The elevation of intracellular Ca^{2+} ($[Ca^{2+}]_i$) causes the activation of transient receptor potential channel M5 (TRPM5) (Perez et al., 2002; Zhang et al., 2007). Opening of this channel allows monovalent cations entry causing depolarization of plasma membrane and action

potential generation (Vandenbeuch & Kinnamon, 2009; Yoshida et al., 2009a). The outcome is the release of ATP through gap junction hemichannels, most likely composed of Pannexin-1 [Fig.5] (Huang et al., 2007). There are many evidence favoring hypothesis of hemichannels composed in Panx-1, for instance, it is highly expressed in TRCs, these hemichannels are gated by elevation of intracellular Ca^{2+} and Panx1-selective agonists block ATP release after taste stimulation (Romanov et al., 2007; Locovei et al., 2006; Dando & Roper, 2009).

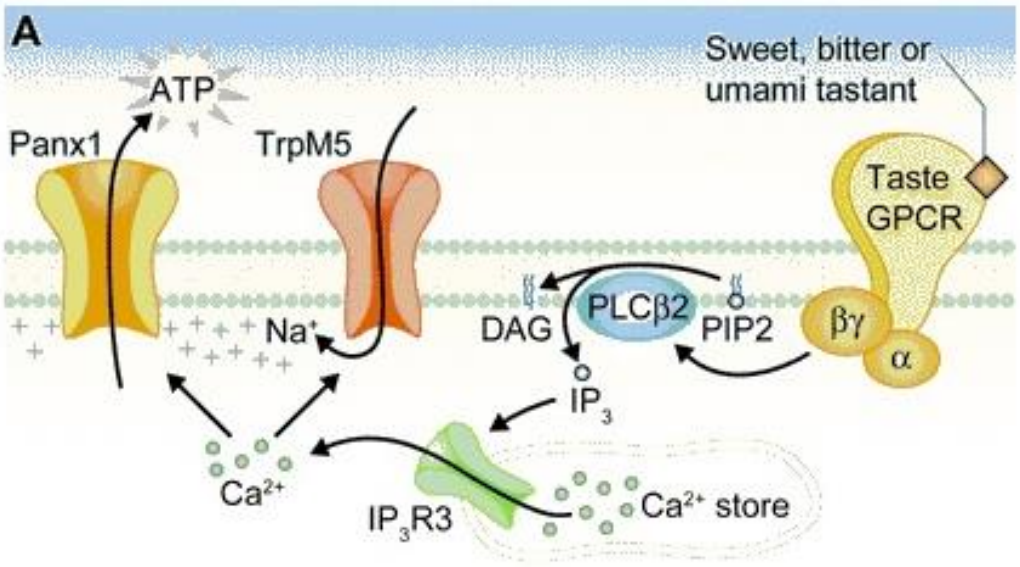

Figure 5: Signal cascade occurring in Type II cells. When tastants bind the specific receptor, βγ-subunits activate PLCβ2 which catalyzes formation of IP_3. The latter binds IP_3 receptors on endoplasmic reticulum leading to release of Ca^{2+} from internal stores. Elevation of $[Ca^{2+}]_i$ actives TRPM5 causing entry of Na^+ and membrane depolarization. Ca^{2+} activates also Pannexin-1 channel through which ATP is released (from Chaudhari & Roper, 2010)

1.3 Taste genetic

Vertebrates differ in Tas2Rs genes, for instance chickens have three genes, humans 25 and mice 35 (Shi & Zhang, 2006). The human genes locate in four chromosomal loci (Adler et al., 2000; Bufe et al., 2002; Meyerhof, 2005). A single gene (TAS2R1) is present on the short arm of chromosome 5. Two loci are

present on the chromosome 7, first consisting in the TAS2R16 and the other in a cluster of eight genes. The remaining genes locate on the short arm of chromosome 12. TAS2Rs genes are known to show extensive genetic variation, including several single nucleotide polymorphism (SNPs), insels and copy number variation. In particular, SNPs are responsible for coding over 151 different haplotypes suggesting that at least some of them may also be functionally different (Kim et al., 2005; Pronin et al., 2007).

Despite the small number of genes, humans can detect numerous bitter compounds, likely due to the large amount of polymorphism and high level of variability between TAS2Rs. Indeed they can share 17 % up to 90 % sequence identity. In general we could say that TAS2Rs respond to several bitter compounds and that a bitter chemical usually activates many receptors. This is possible due to the different receptive ranges of the different TAS2Rs: some being more broadly tunes, thus able to bind a wide array of different compounds, some being more narrowly tuned, able to bind only few possible structurally related compound, even though most of the receptors shows an intermediate degree of promiscuity (Meyerhof et al., 2010).

1.4 Aim of the project

The receptive range of TAS2Rs has been studied using heterologous expression system and calcium imaging experiments in human embryonic kidney 293 cells (HEK293T) stably expressing the chimeric G protein α subunit, Gα16-gust44, a chimeric subunit shown to be very effective in coupling the receptor in such a heterologous system (Chandrashekar et al., 2000; Bufe et al., 2002; Meyerhof et al., 2010; Ueda et al., 2003). To date 21 out of 25 receptors have been deorphanized, but four receptors are still orphan and some are notoriously poor responders, making further investigations difficult. Furthermore, TAS2Rs are known to be poorly expressed on the membrane in heterologous system, thus they do not always show a feasible signal. Indeed, although some receptors give a strong signal with one tastant, the same receptors could give a lower signal with other molecules, or some receptors may give low signal *per se*, if any (Meyerhof et

al., 2010). These limitations raised the necessity to find a way to enhance the Ca^{2+} signal, the readout of the response of TAS2Rs in presence of different tastants. One way to improve the overall outcome might be to provide the above cell line with additional components. A good candidate could be Transient Receptor Potential channel M5 (TRPM5), but being this channel permeable only to monovalent cations it is not suitable for a Ca^{2+} readout (Zhang et al., 2007). Anyway, TRPM5 provide a useful model to improve the heterologous system. Furthermore, mouse TRPC2 is involved in extracellular Ca^{2+} entry through PLC-signaling in vomeronasal organ (Zhang et al., 2010) [Fig.6]. In humans, TRPC2 is a pseudogene, but it still helps useful suggestion. TRPC1 is the archetype of classical TRP channels and is thought to be activated by the same PLC pattern and to be Ca^{2+} permeable, as well (Minke, 2001).

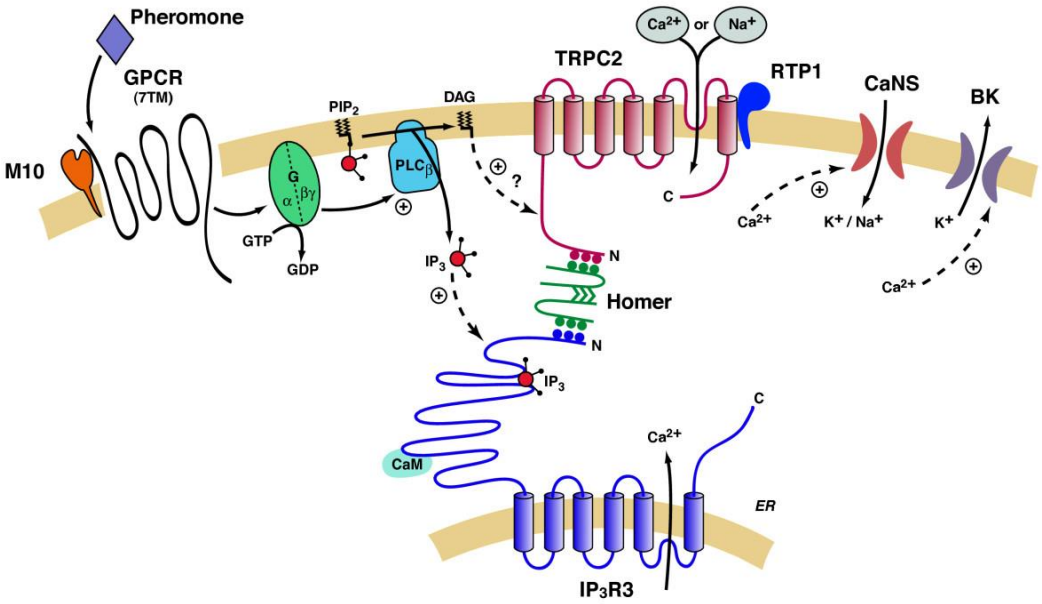

Figure 6: Schematic of the hypothetical vomeronasal organ transduction model. Binding of pheromones to related G protein-coupled receptors actives PLCβ through βγ subunits. PLCβ hydrolyzes PIP_2 producing IP_3 that binds IP_3 receptors opening internal stores and releasing Ca^{2+}. Diacylglycerol is thought to activate TRPC2 allowing entry of cations and thus depolarization of cells (from Mast et al., 2010).

Transient receptor potential (TRP) channels are a group of unique ion channels that serve as cellular sensors for a variety of stimuli, as temperature, taste and

pain. These channels are identified by their homology and it is possible to classify them into several subfamilies: TRPC (canonical), TRPM (melastatin), TRPP (polycystin), TRPV (vanilloid), TRPA (ankyrin), TRPML (mucolipin) (Clapham et al., 2001; Clapham, 2003). The first TRP channel was discovered in a mutant strain of *Drosophila melanogaster* which lacked the functional *trp* gene with consequential impairment in the fly's visual system. TRPC family is the most related to the *Drosophila* TRP channels and comprises seven subunits that can assemble into homotetrameric and also in heteromeric channels (Hofmann et al., 2002; Schaefer, 2005). For instance, TRPC1 can assemble with TRPC3, TRPC4 and TRPC5 (Liu et al., 2005; Gudermann et al., 2004; Strubing et al., 2001). All TRP channels are expected to have six-transmembrane polypeptide chains that assemble as tetramers to form cation-permeable pores. Both the N- and C-terminal are intracellular, with multiple N-terminal ankyrin repeats. The gate and selectivity filter are formed by the segments S5 and S6 facing the center of channel. Cations are selected for permeation by the extracellular loop [Fig.7]. All the TRPC channels are not selective with low Ca^{2+} permeability (Parekh & Penner, 1997).

TRPC1 was the first mammalian homologous of *Drosophila* identified (Zhu et al., 1995; Wes et al., 1995) and cloned in heterologous system in order to study its activity (Zitt et al., 1996). In this study permeability to cations was demonstrated as well as activation by Ca^{2+} release from ER stores. This event links TRPC1 to TAS2Rs, since the latter, like stated above, lead to emptying of internal stores, then the consequential increase of $[Ca^{2+}]_i$.

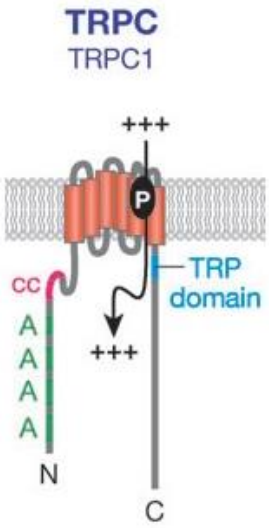

Figure 7: Structure of TRPC1. Transmembrane domains are represented by vertical rectangles, P indicates the pore loops allowing cations entry, CC the coiled-coil domain. Other shown domains are ankyrin repeats (A) and TRP domain (from Venkatachalam & Montell, 2007).

This common feature brought us to choose TRPC1 as useful tool to overcome the limitations described above. TRPC1 cDNA sequence was cloned in an eukaryotic expression vector, with the aim of enhancing Ca^{2+} signal in a cellular model of bitter taste transduction. We started from an extract of fetal human brain mRNA to obtain the cDNA of TRPC1 (Wes et al., 1995; Zhu et al., 1995; Zitt et al., 1996). cDNA was then cloned in an expression vector and HEK293T Gα16gust44 cells, one of the most successful system to characterize the TAS2Rs because very efficient in driving the signal transduction cascade subsequent to bitter receptor activation, have been transiently co-transfected with both TRPC1 and a TAS2R, or the TAS2R alone. Using a fluorescent probe able to bind to intracellular Ca^{2+} and a fluorometric imaging plate reader, Ca^{2+} signals elicited by bitter compounds application were measured, both on cells exclusively transfected with a TAS2R and on cells co-transfected with TRPC1.

We had different results with diverse TAS2Rs, for instance with TAS2R14 and TAS2R43 the signal detected in co-transfected cells was higher than signal in cells transfected only with taste receptor. On the other hand with TAS2R10 we had the opposite result, with a higher signal in cells expressing only the receptor.

Enhancing Ca^{2+} signal in the current assay could allow us to deorphanize receptors whose tastants are not yet known merely because of low signal in the system, or to find others molecules that activate a given TAS2R, thus widening/expanding the range of activators of that receptor. A further characterization of TAS2Rs receptive ranges and activation modulation is of primary interest for food/nutritional and taste sciences, as well for the food/taste industry. Moreover, it could be possible to study inhibitors in those receptors that have strong signal with a tastant and low signal with other substance(s). In this case pharmacological industry could be interested in finding inhibitors for those bitter substances used in medicines, to make better-tasting drugs improving pediatric adherence to drugs therapy (Mennella et al., 2013). Finally, food industry could be interested in using bitter inhibitors “to virtually eliminate bitterness from the world” (Drewnowsky & Gomez-Carneros, 2000).

2. MATERIALS AND METHODS

2.1 Bitter compounds

Bitter compounds were purchased from Sigma Aldrich Chemie Gmbh (Taufkirchen, Germany). The substances were both dissolved and administered in a mixture of dimethyl sulfoxide (DMSO) and buffer C1 (see section 2.4), not exceeding a final DMSO concentration of 0.1% to avoid noxious effects on the cells.

We chose to transfect hTAS2R10, hTAS2R14, hTAS2R43, thus we used strychnine to activate hTAS2R10 and aristolochic acid that binds both hTAS2R14 and hTAS2R43 (Bufe et al., 2002; Behrens et al., 2004; Kuhn et al., 2004). Both the substances were used in two different concentrations, the higher known to elicit a robust response by the relative receptor:

Aristolochic Acid (TAS2R14)	Aristolochic Acid (TAS2R43)	Strychnine (TAS2R10)
1 µM	0.1 µM	30 µM
3 µM	0.3 µM	100 µM

Bitter-tastant solutions have been prepared 3-times more concentrated than the indicated concentrations because FLIPR device adds 50 µl to 100 µl volume present in every well, thus diluting three times and obtaining the correct concentrations.

2.2 Isolation of TRPC1 cDNA sequence and creation of expression vector

Retrotranscription has been performed from fetal human brain mRNA extract (Wes et al 1995, Zhu et al., 1995; Zitt et al., 1996). DNAase I (Invitrogen) has been used to remove DNA contamination from RNAs.

DNA digestion mix	
RNA	1.5 µg (volume differs on the basis of RNA concentration)
RNAase Inhibitor Ribolock 40 U/µl (Fermentas)	0.25 µl
Dithiothreitol (DTT) 10mM (Invitrogen)	1.5 µl
10X DNAase I Buffer (Invitrogen)	1.5 µl
DNAase I 2 U/µl (Invitrogen)	1 µl
Water	Up to 15 µl final volume

The digestion has been performed for 30 minutes at room temperature, following the manufacturer's instructions. We added 1.25 µl of EDTA 25 mM and solution has been incubated 10 min at 65°C. Briefly on ice. The product has been divided in two tubes, one for negative control without retrotranscriptase (-RT).
For the cDNA synthesis:

cDNA synthesis initial mix (+RT reaction)	
DNA digestion mix	10 µl
Random primer 3000 ng/ µl (Invitrogen)	1 µl (Final concentration = 250 ng/ µl)
dNTPs 10mM	1 µl

–RT reaction has been performed with half of the volumes listed above. The solution has been incubated for 5 min at 65°C, then briefly on ice.

After that, we added to previous solution:

cDNA synthesis final mix (+RT reaction)	
$MgCl_2$ 25 mM	0.85 µl
DTT 100 mM	1.9 µl
RNAase Inhibitor Ribolock	0.25 µl
5X Reverse Transcriptase Buffer	4 µl
Reverse Transcriptase SuperScript II 200U/µl(Invitrogen)	1 µl

The same reaction has been performed with half of previous quantities and omitting reverse transcriptase for –RT control. Both the mixes have been incubated 10 min at room temperature, then 50 min at 42°C, finally 15 min at 70°C. The solutions have been centrifuged and put briefly on ice. In the end, we reached the final volume of 100 µl for +RT solution and 62.5 µl for –RT reaction, with autoclaved, distilled water.

We performed a control Polymerase Chain Reaction (PCR) for housekeeping gene Glyceraldehyde 3-phosphate dehydrogenase (GAPDH) to verify the success of retrotranscription. Cycling parameter were as follows:

GAPDH PCR protocol			
First denaturation	95°C	1 min	
Denaturation	95°C	30 sec	29 cycles
Annealing	58°C	30 sec	
Elongation	68°C	1 min	
Final annealing	58°C	10 min	
Final elongation	68°C	10 min	
Storing	4°C	∞	

GAPDH PCR reaction mix	
cDNA synthesis final mix	2.5 µl
Primer Forward (10 mM)	2 µl
Primer Reverse (10 mM)	2 µl
dNTPs 2.5 µM	1 µl
10x Advantage 2 PCR Buffer	5 µl
50X Advantage 2 Polymerase Mix (Clontech Laboratories)	0.7 µl
Water	36.8 µl

The used primers for GAPDH PCR were the forward 5'-ACCACAGTCCATGCCATCAC-3' and the reverse 5'-TCCCACCACCCTGTTGCTGTA-3', both purchased from Clontech. These are internal primers amplifying a sequence of ~500 bp.

PCR products have been checked by agarose gel 1%.

cDNA sequence PCR has been performed with sequence-specific primers. In forward primer 5'-ACGATATCCACCATGATGGCGGCCCTGTACCCGA-3' (melting temperature T_m = 77°C), restriction site of enzyme EcoRV (GATATC) as well as Kozak sequence (CCACC), has been included at 5' terminal restriction site. The reverse primer 5'-GTTATTGTCTAGGTTTTCTGATATAACGTATTGAACGCCGGCGCT-3' contained the NotI restriction site (GCGGCC). Primers have been purchased from Eurofins Scientific. The used protocol was:

TRPC1 cDNA PCR protocol			
First denaturation	95°C	1 min	
Denaturation	95°C	30 sec	35 cycles
Annealing	66°C	2 min 30 sec	
Elongation	68°C	2 min 30 sec	
Final elongation	68°C	7 min	
Storing	4°C	∞	

TRPC1 cDNA PCR reaction mix	
cDNA synthesis final mix	2 µl
Primer Forward (10 mM)	1 µl
Primer Reverse (10 mM)	1 µl
dNTPs 2.5 µM	0.5 µl
10x Advantage 2 PCR Buffer	2.5µl
50X Advantage 2 Polymerase Mix (Clontech Laboratories)	0.4 µl
Water	17.6 µl

The fragment has been checked by agarose gel 1% and extraction of the cDNA fragment from the electrophoresis gel was performed with QIAquick Gel extraction kit (Qiagen). We eluted in 50 µl of water.

We first submitted TRPC1 fragment to TOPO TA cloning reaction (Life Technologies) for 30 minutes at room temperature. On a final volume of 6 µl we used 4 µl of cDNA solution, 1µl of salt solution and 1µl of TOPO vector. One Shot TOP10 chemically competent *E. coli* cells (Invitrogen) have been transformed with 2 µl of TOPO cloning solution. The cells have been incubated 30 minutes on ice, a heat-shock for 30 s at 42°C was performed and the tube was cooled on ice for 2 min. Then we added 250 µl of S.O.C. medium warmed at room temperature to the transformed cells. Pre-growth has been performed for 1 hour at 37°C, shaking the vial horizontally. Samples were spread on pre-warmed solid medium plates added with ampicillin 100 µg/ml and plates were cultured at 37°C overnight.

The next day grown colonies were picked and amplified in Liquid Broth (LB) medium pH 7.4 with ampicillin 100 µg/ml at 37°C overnight. In order to collect TOPO vector/TRPC1 constructs, MINI preparation reaction of the grown colonies were performed with JETQUICK Plasmid purification spin kit (Genomed).

In order to confirm successful subcloning of TRPC1 cDNA fragment, the purified plasmids have been digested with restriction enzyme EcoRI (20,000 units/ml, Fermentas) giving a specific restriction pattern if the fragment has been inserted in vector. Samples showing expected EcoRI restriction pattern were double digested

with the EcoRV (20,000 units/ml) and NotI (10,000 units/ml) restriction enzymes (New England BioLabs). Both digestions have been performed for 1 hour at 37°C. On a final volume of 10 µl we used 0.3 µl of each restriction enzyme, 1 µl of relative 10X buffer and ~ 250 ng of DNA.

Samples showing expected restriction pattern, as well as pcDNA 3.1/Zeo^{+} (Invitrogen), were digested overnight at 37°C with restriction enzymes EcoRV and NotI in order to obtain fragments and pcDNA complementary with each other. 3 µg of DNA were digested with 3 µl of each enzyme and 2.5 µl of 10X buffer, on a final volume of 25 µl.

In order to eliminate contamination from cDNA fragments and pcDNA solutions, these were run in agarose gel 1% and then extracted from gel as above. In order to clone the fragment in the expression plasmid, the cDNA and pcDNA were ligated with T4 DNA Ligase (New England BioLabs) overnight at 16°C. We used 50 ng of pcDNA and two different ratio between plasmid and digested fragment, to optimize cells transformation.

The required volume of cDNA has been calculated as follows:

$$\frac{bp\ cDNA\ \times\ ng\ plasmid}{bp\ plasmid} \times ratio = ng\ fragment => \frac{ng\ cDNA}{[cDNA]} =\ \mu l\ cDNA$$

Ligation mix		
Ratio	1:2	1:3
Plasmid [23 ng/µl]	2.17 µl	2.17 µl
cDNA	From formula above	
10X T4 DNA ligase Buffer	2 µl	2 µl
T4 DNA ligase 400 U/ µl	1 µl	1 µl
water	Up to 20 µl	Up to 20 µl

One Shot TOP10 chemically competent *E. coli* cells were transformed (see above for protocol) with 5 µl of ligation solution and then cultured on solid medium plates, added with ampicillin, overnight at 37°. Once again, the next day plasmid

purification has been performed (see above) and two control digestions have been carried out on positive samples with EcoRI, EcoRV and NotI (see above for quantities).

Positive samples for correct TRPC1 sequence, from both TOPO cloning reaction and cloning in pcDNA 3.1/Zeo$^+$, have been verified for EcoRV and NotI restriction sites, for Kozak sequence and for a portion of the pcDNA 3.1/Zeo$^+$ up and downstream the cDNA insert by direct sequencing by Eurofins Scientific. The correct constructs were used to transiently transfect HEK293T.

2.3 Functional expression

Human Embryonic Kidney (HEK)-293T cells, already stably expressing the chimeric G-protein subunit Gα16gust44, were transiently transfected with obtained constructs. This cell line stably express human Gα16 at the N-terminus fused with 44 amino acids of human α-gustducin (Ueda et al., 2003). This chimera is very effective in coupling to hTAS2Rs (Kuhn et al., 2004; Brockhoff et al., 2010). Plasmids carrying TAS2Rs sequence are based on pcDNA5/FRT (Invitrogen) and they present a sequence of the rat somatostatin type 3 receptor at the N-terminus of the recombinant polypeptide in order to improve membrane targeting of the receptors and a herpes simplex virus glycoprotein D (HSV) epitope at its C-terminal, necessary for immunocytochemical expression analysis (Bufe et al., 2002).

The first day HEK293T cells were plated in 96-wells dark plate, pre-coated with 10 µg/ml Poly-D-lysine, at a density of 1-2 * 10^4/well.

After ~24 hours cells were transfected with the same quantity (75 ng) of TRPC1 cDNA construct and TAS2Rs cDNA constructs, or with TAS2Rs cDNA constructs and mock (empty vector used as negative control) or only with mock, to a final quantity of 150 ng of DNA/well. This is fundamental to have a comparable amount of cells expressing TAS2R and thus comparable signals between test and control cells.

The mixtures of plasmids have been incubated in 12.5 µl/well serum-free medium for 5 minutes at room temperature. 12.5 µl/well of mix of Lipofectamine 2000

(Invitrogen) and serum-free medium were added to the DNA mixtures and incubated for 20 minutes at room temperature.

Plates have been washed and filled with 50 µl/well of serum-free medium and 24 µl of corresponding transfection solution were further added in every well. After 3-5 hours of incubation at 37°C serum-free medium was replaced by 100 µl/well complete DMEM medium. Calcium analysis was performed 24 hours after the transfection.

2.4 Calcium imaging

24-26 hours after transfection, cells were loaded with calcium-sensitive dye Fluo-4-AM (Life Technologies), in serum-free culture medium. To minimize the loss of dye from the cells, Probenecid (Invitrogen), an inhibitor of organic anion transport, was added at concentration of 2.5 mM. To 5.5 ml DMEM medium/96-well plate, 5.5 µl Fluo-4-AM (50 µg of dye diluted in 22 µl DMSO, thus we obtain a final concentration of 2.5 µg/ml for every plate) and 55 µl Probenecid were added. Plates were washed and every well was filled with 50 µl of solution with dye. 96-well plates were incubated at 37°C for 1 hour. 3 washes with C1 buffer (130 mM NaCl, 5 mM KCl, 10 mM HEPES, 2 mM $CaCl_2$, 10 mM glucose, pH 7.4) at interval of 20 minutes followed. Between washes plates were incubated at room temperature in the dark. The last wash was performed right before Ca^{2+} analysis. Cellular Ca^{2+} signal was recorded at 510 nm following excitation at 488 nm using an automated Fluorometric Imaging Plate Reader (FLIPR, Molecular Devices), after application of bitter compound. A second application of 100 nM somatostatin 14 (Bachem), activating the endogenous somatostatin receptor type 2 known to lead to [Ca^{2+}] variations, assessed functionality of Ca^{2+} signaling.

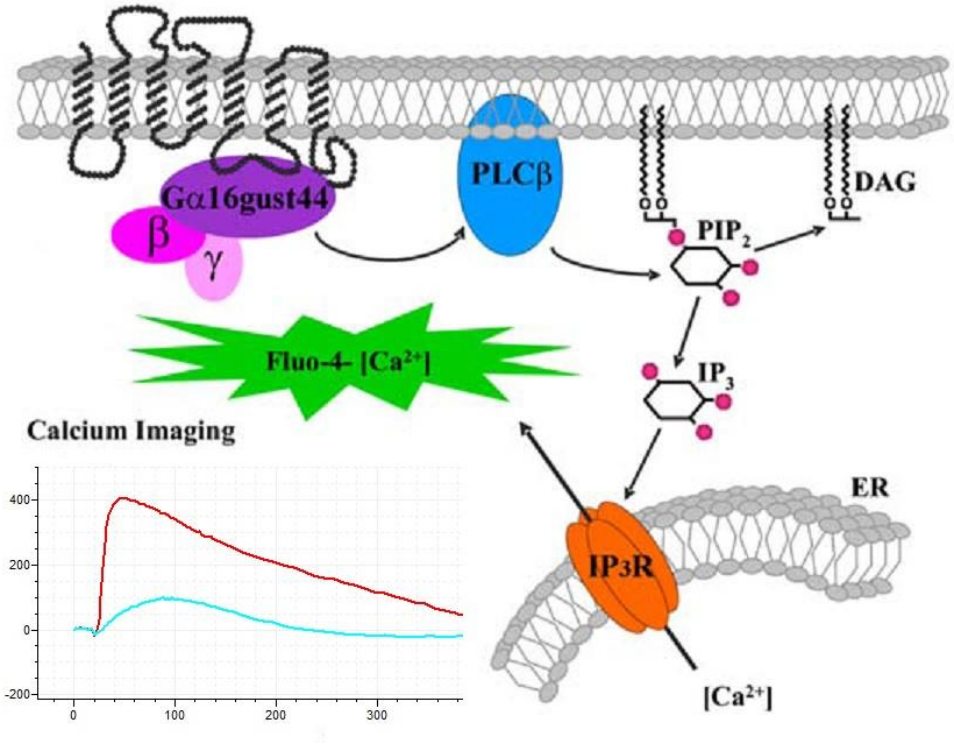

Figure 8: Ca^{2+} imaging in a model of taste transduction. The chimeric G α-subunit, after administration of substance on related receptor, allows activation of PLCβ leading to hydrolyzation of PIP_2 and to IP_3 production. IP_3 receptors are activated and allow release of Ca^{2+} from ER stores. Fluo-4-AM binds Ca^{2+} located in cytosol emitting a characteristic fluorescence detected by a CCD camera and displayed in real time by the software. (Anne Brockhoff ©)

Data were collected from at least 3 independent experiments performed in duplicate, extracted with ScreenWorks 3.1 software and analyzed by Microsoft Excel (2007). The maximal fluorescence after administration of compound was corrected for and normalized to background fluorescence ($\Delta F/F = (F - F_0)/F_0$). Baseline noise was subtracted.

3. RESULTS AND DISCUSSION

3.1 Isolating and cloning of TRPC1 cDNA

Taste receptors are known to be poorly expressed in heterologous system, even more they respond with high variability against relative compound and some receptors have low signal *per se* (Meyerhof et al., 2010). Both these reasons cause low Ca^{2+} signal in calcium imaging functional assay, thus making deeper investigation difficult. This raised the necessity to overcome these limitations. In order to find a useful tool able to improve the intracellular Ca^{2+} concentration, attention has been focused on those channels that could be involved in Store-Operated Ca^{2+} entry (SOCE), a Ca^{2+} entry pathway through a dedicated channel activated by depletion of internal stores. Implication of TRPM5 in taste transduction, activated by increasing of $[Ca^{2+}]_i$, shed a light on TRP channels (Hofmann et al., 2003; Prawitt et al., 2003). Moreover, the role of TRPC2 in vomeronasal organ (VNO) in mice confirmed this idea. Indeed pheromones receptors (VR) in VNO are GPCR activating PLCβ2 that hydrolyzes phosphatidylinositol 4, 5–bisphosphate (PIP_2) in plasma membrane producing diacylglycerol (DAG) and IP_3. TRPC2 has been proposed to be activated by DAG leading to increase of $[Ca^{2+}]_i$, [Fig.6] (Lucas et al., 2003). While in humans TRPC2 is a pseudogene, TRPC1 has been the first TRP channel identified in humans and resulted functional when expressed in heterologous system (Wes et al., 1995; Zitt et al., 1996). Several studies have demonstrated that TRPC1 is involved in SOCE and is activated by increase of $[Ca^{2+}]_i$ released from internal stores (Wu et al., 2000; Wes et al., 1995; Liu et al., 2003). It has been reported that TRPC1 is expressed in a variety of tissue, including brain where for instance seems to be responsible of an excitatory postsynaptic current in Purkinje cells (Wes et al., 1995; Kim et al., 2003). Hence, we started from mRNA extracts of fetal human brain, on which a reverse transcription was performed, in order to amplify TRPC1 cDNA. Reverse transcription was validated through PCR reaction for housekeeping Glyceraldehyde 3-phosphate dehydrogenase (GAPDH) gene, constitutively expressed in most tissues, thus commonly used as control. The primers here used amplify a region of 450 bp of the sequence. Presence and

concentration of the fragment indicate successful reverse transcription and the quality of mRNA extract. It is possible to notice the amplified fragment in the first lane and negative control in the second lane. [Fig.9].

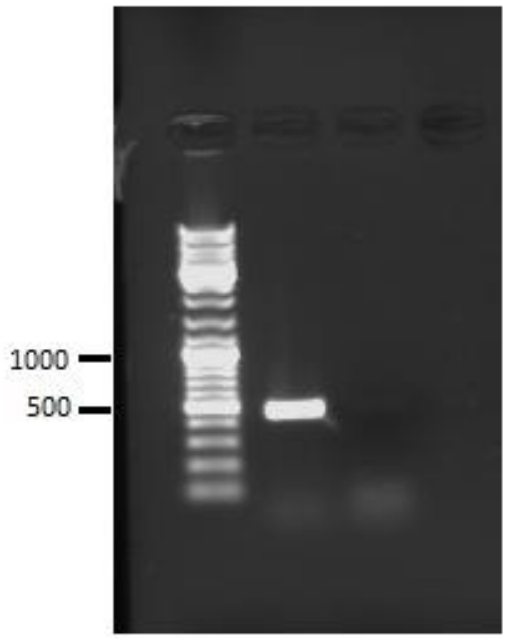

Figure 9: Agarose gel run of PCR for GAPDH. The primers amplify a region of 450 bp. GeneRuler Marker has been used as molecular weight on the left of the gel.

From reverse transcription, TRPC1 cDNA was amplified through a PCR reaction with primers designed on gene sequence deposited in PubMed data base (NCBI Reference Sequence: NM_001251845.1). The protocol described in section 2.2 provided a 2382 bp long fragment and an aspecific fragment [Fig.10]. A gel extraction was performed in order to isolate the right PCR product and avoid the aspecific. Length-correct fragment was used for a TOPO cloning reaction with the aim to obtain a larger quantity of TRPC1 product. This passage was necessary since the concentration of PCR product was not abundant enough for subsequent steps of gel extraction and purification, prior directional cloning. Thus, subcloning in TOPO vector provided a higher cDNA concentration useful for subsequent steps and cloning in an eukaryotic expression vector.

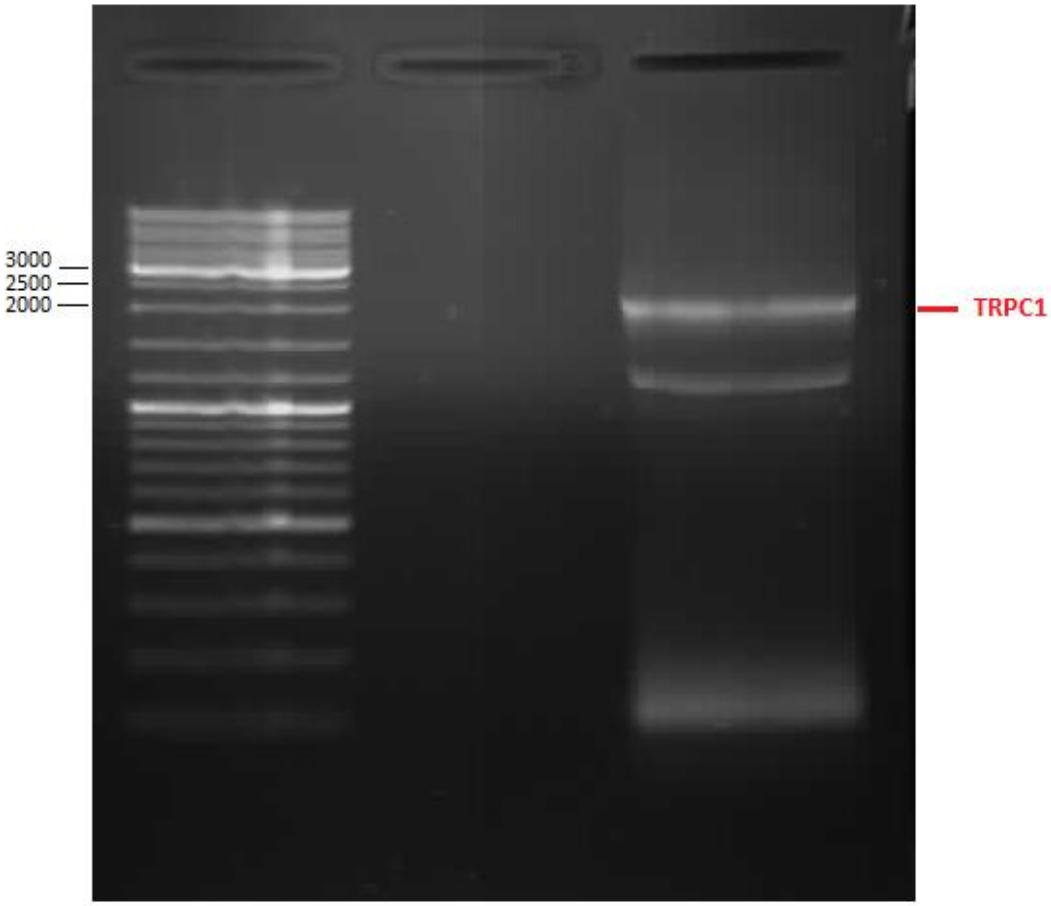

Figure 10: Agarose gel run of PCR for TRPC1 cDNA. Gel shows TRPC1 cDNA at 2382 bp. An aspecific fragment can be seen under TRPC1 fragment, hence the latter has been extracted from the gel. GeneRuler Marker has been used as molecular weight on the left side of the gel.

After plasmid purification from colonies transformed with TOPO cloning reaction mix, presence of TRPC1 cDNA has been confirmed through two control digestions, using the restriction enzymes EcoRI, NotI and EcoRV whose restriction sites were included upstream and downstream of cDNA through PCR amplification from product of reverse transcription (see section 2.2). Thus, while the enzymes EcoRV and NotI excise cDNA sequence from plasmid, EcoRI enzyme provides specific restriction pattern, since TOPO vector contains 2 EcoRI restriction sites upstream and downstream multicloning site (MCS) [Fig. 11 A] and TRPC1 sequence contains 4 EcoRI sites [Fig.11 B]. Hence, we expected six fragments: 3931 bp for TOPO vector and five fragments of different length from cDNA TRPC1 (444 bp, 314 bp, 74 bp, 555 bp, 995 bp).

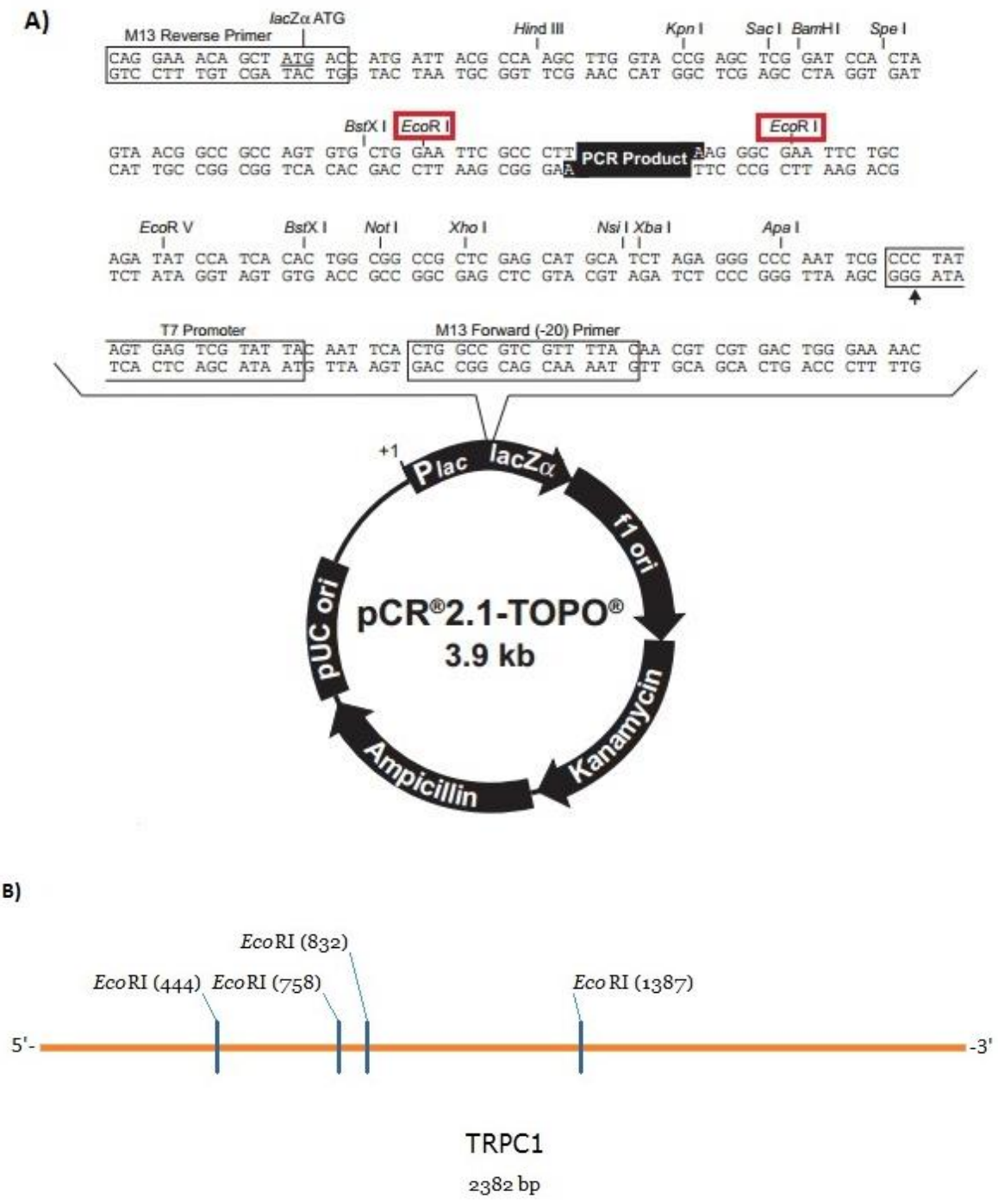

Figure 11: (A) pCR 2.1 TOPO map. EcoRI sites are red squared (Life Technologies). **(B)** Positions of EcoRI sites on TRPC1 Isoform 1 sequence.

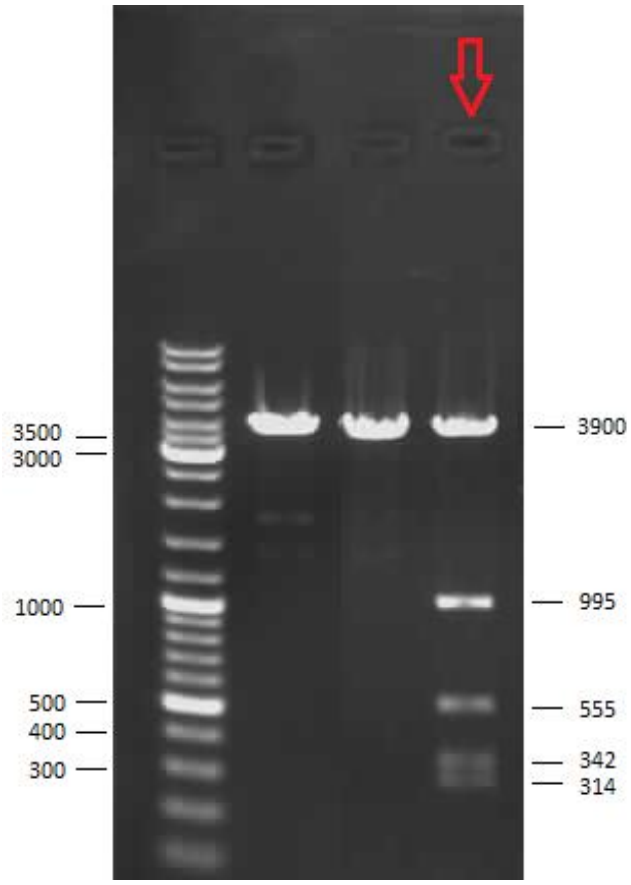

Figure 12: Agarose gel run of EcoRI control digestion of TOPO vector/TRPC1 constructs. Red arrow shows the sample with the correct restriction pattern for EcoRI digestion. GeneRuler Marker has been used as molecular weight on both sides of the gel.

The results of control digestion with EcoRI was checked through an agarose gel run. Fig.12 shows the empty vectors in the first two lanes, while in the third there is an example of sample showing the correct restriction pattern, even if in place of expected 444 bp fragment we obtained a shorter fragment. To validate TRPC1 cDNA the sequence has been checked through a direct sequencing and was not found corresponding to the TRPC1 Isoform 1 deposited sequence [NCBI Reference Sequence: NM_001251845.1] (data not shown). This unexpected result brought us to inquire into both databases and literature about TRP channels. We found that TRPC1 is expressed in more than one splice variant (Zitt et al., 1996; Ong et al., 2013). In particular TRPC1 variant 2 lacks of 102 bp corresponding to exon 2. Comparing this isoform with the variant 1 we turned out that this

alternative splicing is responsible of the shorter fragment obtained from EcoRI digestion [Fig.13]. TRPC1 sequence checked by direct sequencing was confirmed to be corresponding to human TRPC1 variant 2 [NCBI Reference Sequence: NM_003304.4]. Despite lacking 102 bp encoding the amino acids 109-143, this variant was reported to be still functional (Zitt et al., 1996).

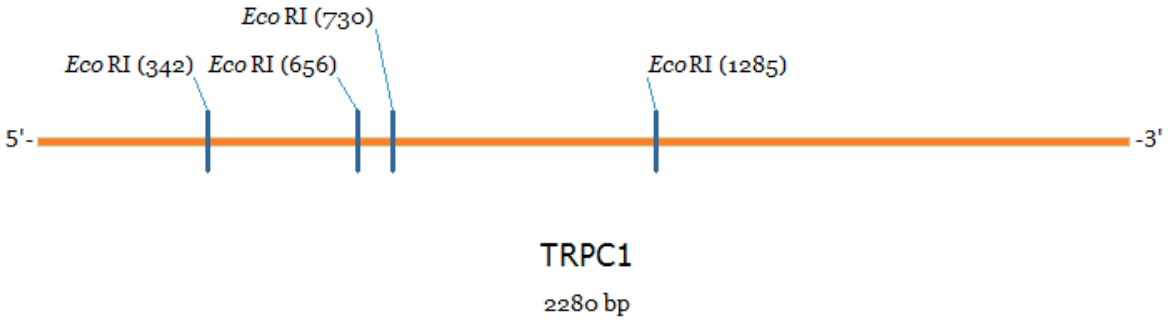

Figure 13: EcoRI sites on TRPC1 Isoform 2 sequence.

Afterwards, EcoRV and NotI double digestion has also been performed on those samples having a correct EcoRI restriction pattern and was possible to notice the 2280 bp fragment excised from TOPO vector [Fig 14].

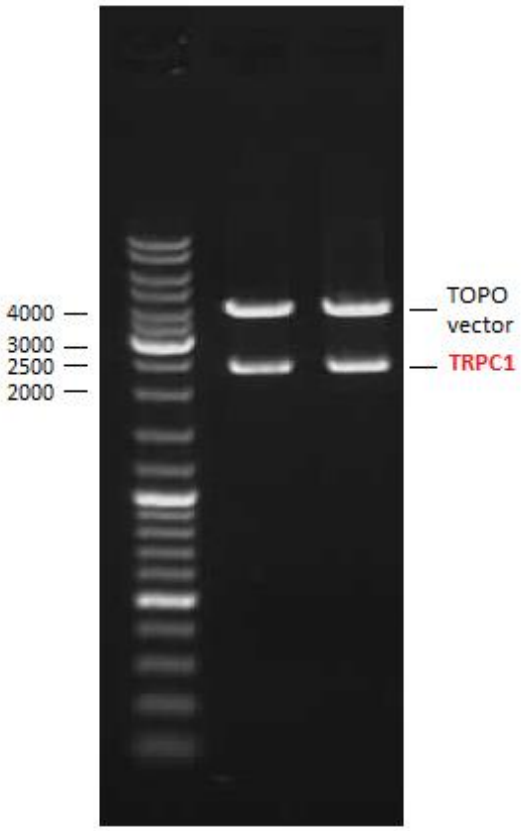

Figure 14: Agarose gel run of EcoRV and NotI control digestion of TOPO vector/TRPC1 construct. These enzymes excide TRPC1 sequence from TOPO vector, thus it is possible to see the bands at 3931 bp corresponding to TOPO plasmid and TRPC1 sequence at 2280 bp. GeneRuler Marker has been used as molecular weight on left side of the gel.

Afterwards TRPC1 sequence has been ligated to the pcDNA 3.1/Zeo^{+} plasmid and One Shot TOP10 chemically competent *E. coli* cells have been transformed. The constructs obtained after a plasmid purification have been checked by control digestion, again with EcoRI.

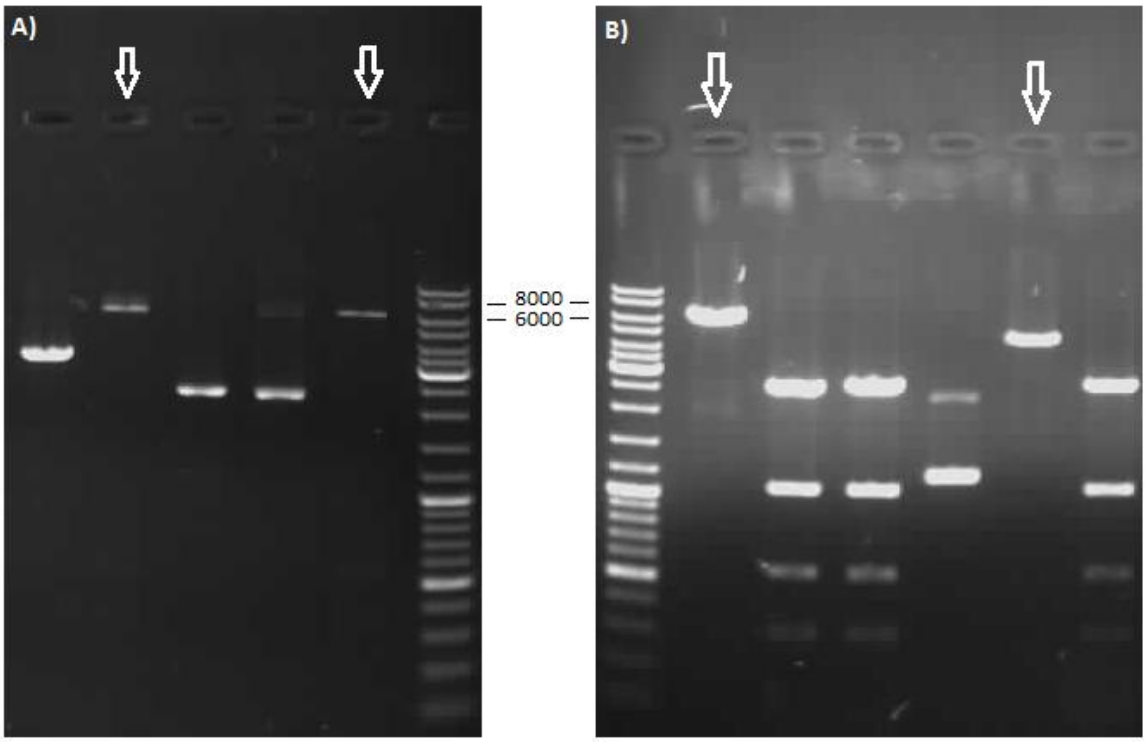

Figure 15: Agarose gel run of EcoRI control digestion of pcDNA 3.1 Zeo^{+}/TRPC1 constructs (A and B). White arrows indicate bands at 7295 bp, comparable to cDNA ligated to pcDNA. No samples showed correct expected restriction pattern (see text for further information). GeneRuler Marker has been used as molecular weight on both sides of the gel.

In this case the results were not as expected, as the characteristic restriction pattern described at p.25, but four samples showed a single ~7300 bp band (white arrows), likely corresponding to linearized expected constructs (2280 + 5015 = 7295 bp) [Fig. 15 A-B]. Probably the EcoRI sites have been methylated by *E.coli* enzymes preventing restriction enzyme's activity. All the other samples showed different digestion patterns not corresponding to any suitable result. Thus, control digestion with EcoRV and NotI has been performed on 7295 bp-long fragment to verify presence of TRPC1 sequence.

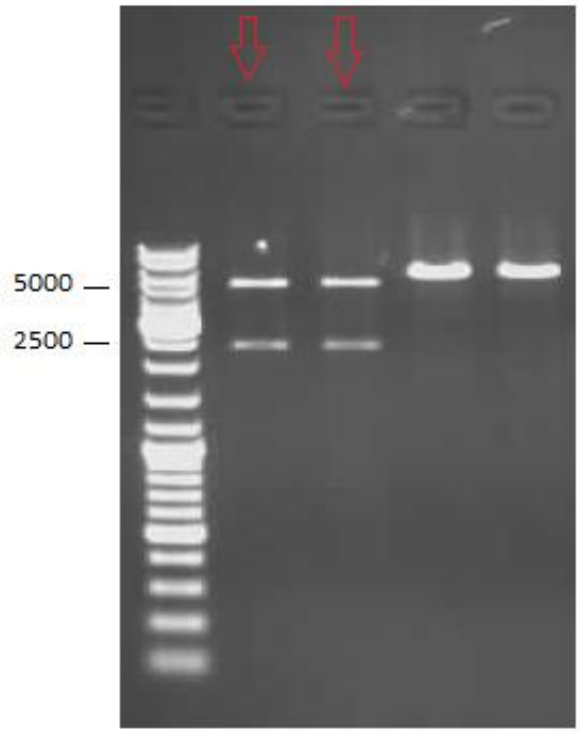

Figure 16: Agarose gel run of EcoRV and NotI control digestion of pcDNA 3.1 Zeo^{+}/TRPC1 construct. Image shows the result of control digestion with enzymes whose restriction sites were included in oligonucleotides used for amplification of TRPC1 cDNA. Only in two samples cDNA has been excised from plasmid (indicated by red arrows), indeed is possible to note a band at 5015 bp corresponding to linearized plasmid, and a band at 2280 bp related to TRPC1 sequence. GeneRuler Marker was used as molecular weight on left side of the gel

In Fig.16 results of control digestion are shown. Only two samples present the excised fragments at 2280 bp and linearized plasmid at 5015 bp (first two lanes), the other two samples probably were partially digested plasmids and they did not contain cDNA fragment, indeed the length of these fragments is slightly higher than empty linearized vector.

The correct constructs were checked by direct sequencing for mutations, for presence of EcoRV and NotI sites, for Kozak sequence, fundamental for eukaryotic translation, for initial ATG codon and TAA stop codon [Fig.17].

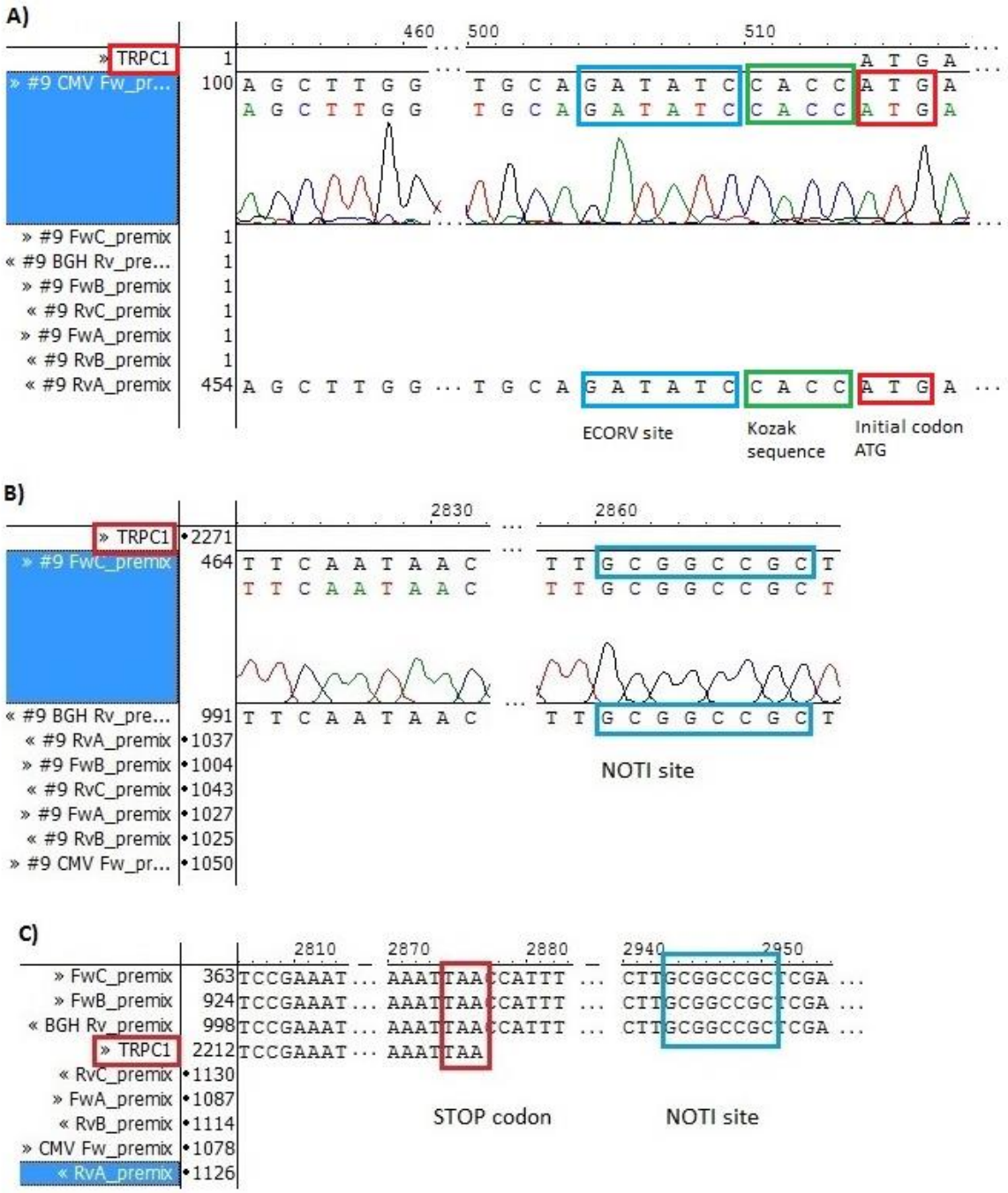

Figure 17: Alignment between directly sequenced constructs and original TRPC1 Isoform 2 deposited sequence (red square) [NCBI Reference Sequence: NM_003304.4]. **(A):** EcoRV site, Kozak sequence used to start eukaryotic translation, and initial ATG codon are highlighted. The chromatogram related to sequence obtained from CMV forward primer is also shown. Absence of background noise represents the correctness of sequencing. **(B):** NotI restriction site is shown downstream of TAA stop codon at cDNA 3'-terminal **(C)**. In **(B)** is also shown chromatogram obtained from sequencing of cDNA using BGH reverse primer. CMV and BGH sequence are located up- and downstream of MCS of plasmid, respectively.

While a sample was highly mutated (data not shown), in the other cDNA sequence a mutation was found in position 1701 bp, corresponding to the third base of triplet coding for amino acid 567. Mutation turned out to be a silent mutation changing TTA in TTG triplet, both coding amino acid Leucine [Fig. 18].

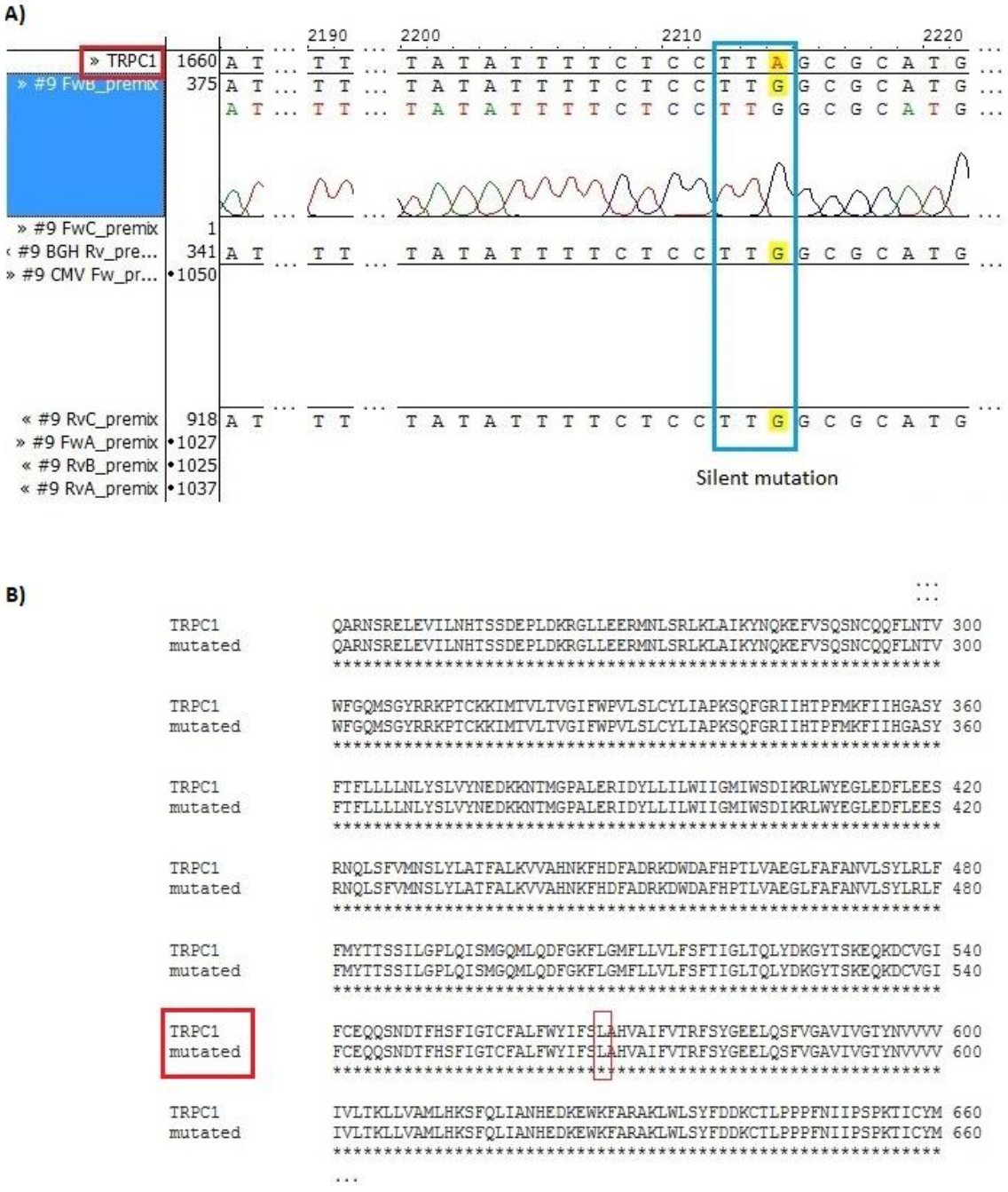

Figure 18: Alignment between sequenced constructs and original TRPC1 Isoform 2 deposited sequence (red square) [NCBI Reference Sequence: NM_003304.4] showing in **(A)** position of mutated base. **(B)** Alignment between amino acid sequence of original TRPC1 (indicated as TRPC1) and the one encoded by the mutated construct (indicated as mutated). The involved amino acid is squared in red and is possible to note that in both sequences is a Leucine.

Sample resulted mutated in position 1701 is also found correct for both restriction sites, Kozak sequence downstream of EcoRI site, initial codon ATG and stop codon TAA upstream of NotI site [Fig.17] and it has been used to transfect HEK293T cells with a TAS2R.

3.2 Calcium imaging and statistical analysis

Cells used as model of taste transduction were Human Embryonic Kidney 293T cells. Since these cells do not possess all the molecules involved in taste transduction cascade this heterologous system have been modified by stably expressing chimeric G-protein α subunit, very effective in coupling with TAS2Rs (Ueda et al., 2003).

The TAS2Rs sequence-carrying constructs were already cloned in expression vector described in Section 2.3. Trying to overcome ineffective membrane targeting, the sequence encoding the first 45 amino acids of rat somatostatin receptor 3 was cloned upstream of coding region, because very efficient in transmembrane targeting (Bufe et al., 2002; Ammon et al., 2002). At 3'-terminal the coding region was cloned with the sequence encoding for Herpes simplex virus Glycoprotein D, useful for subsequent immunocytochemical expression analysis (Bufe et al., 2002).

The choice of TAS2Rs to test fell on those receptors with strong signal against specific compound to verify the effective action of TRPC1 on Ca^{2+} signal. Hence, we chose TAS2R14 and -43, both having a strong signal when stimulated with aristolochic acid (Kuhn et al., 2004; Meyerhof et al., 2010) and for TAS2R10 strychnine has been chosen (Meyerhof et al., 2010; Born et al., 2013). Both the substances are notoriously bitter and also toxic: aristolochic acid is known to have carcinogenic, mutagenic and also nephrotoxic effects, while strychnine is a famous poison being an inhibitor of glycine and acetylcholine receptors in motor neurons (DeBroe, 2012).

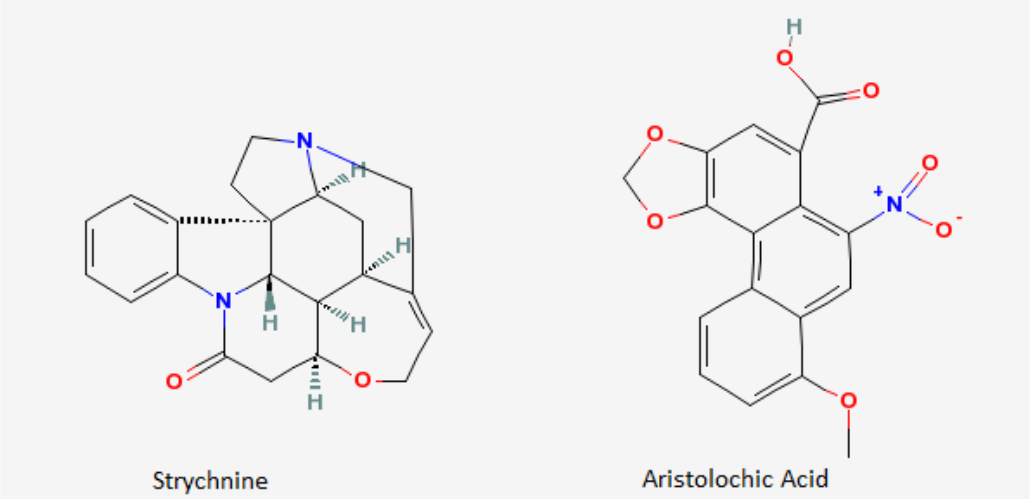

Figure 19: Structures of bitter compound used (from Kuhn et al., 2004).

The 96-well plates were designed to have, in every plate, cells co-transfected with TRPC1 and TAS2R, TAS2R and empty vector and only empty vector as negative control. Every condition was replicated at least two time for a minimum of three experiments.

	1	2	3	4	5	6	7	8	9	10	11	12
A	TAS2R + TRPC1			TAS2R + TRPC1			TAS2R + TRPC1			TAS2R + TRPC1		
B												
C												
D	TAS2R + mock			TAS2R + mock			TAS2R + mock			TAS2R + mock		
E												
F												
G	mock			mock			mock			mock		
H												

Figure 20: Layout of transfection in 96-well plate. Every combination of TAS2R and TRPC1 or mock have been used to transfect 9 wells, while every negative control relative to every combination were 6 wells.

To have preliminary quantitative results about TRPC1 activity, each substance has been tested in two different concentrations. The lower concentration were used to point out possible differences in presence of TRPC1 that could be overlooked by strong signal in case of saturation due to the higher concentration.
After administration of solutions we could observe improved signals already from the real time data of FLIPR for both receptors TAS2R14 and TAS2R43, results that have been confirmed by statistical analysis.

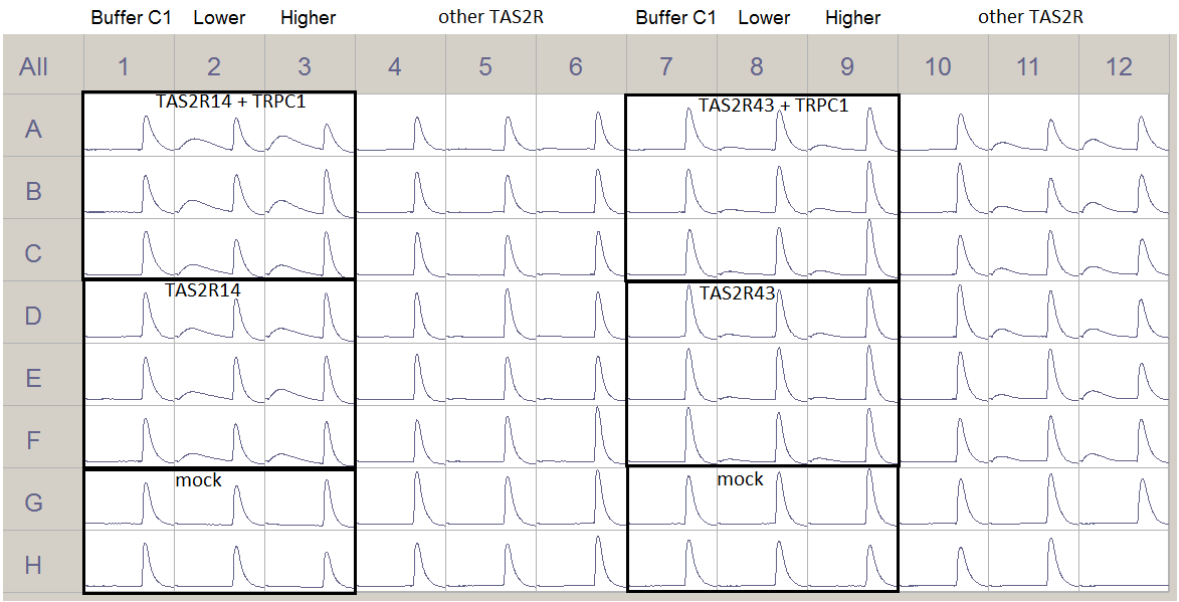

Figure 21: Layout of real-time Ca^{2+} imaging through FLIPR device. Transfection has been performed as shown in **Fig.20**. The columns 1-4-7-10 have been stimulated by C1 buffer. The columns 2-5-8-11 have been stimulated by the lower concentrated solutions of the specific tastant for the TAS2R transfected. The columns 3-6-9-12 have been stimulated by the higher concentrated solutions.

For every experiment we calculated the averages of each experimental condition, these values were then used to obtain a final mean of signal from TRPC1+TAS2R transfected cells and mean of TAS2R+mock transfected cells from at least three independent experiment. These results were analyzed by Student t-test obtaining p-values considered statistically significative if less than 0.05 (p-value < 0.05).
In Fig.22 signals, expressed as percent, relative to experiments of TAS2R14 are reported. It is possible to notice that signal of cell transfected with both TAS2R14

and TRPC1 (blue) is almost 120% with respect to signal of cells exclusively transfected with TAS2R14 (red).

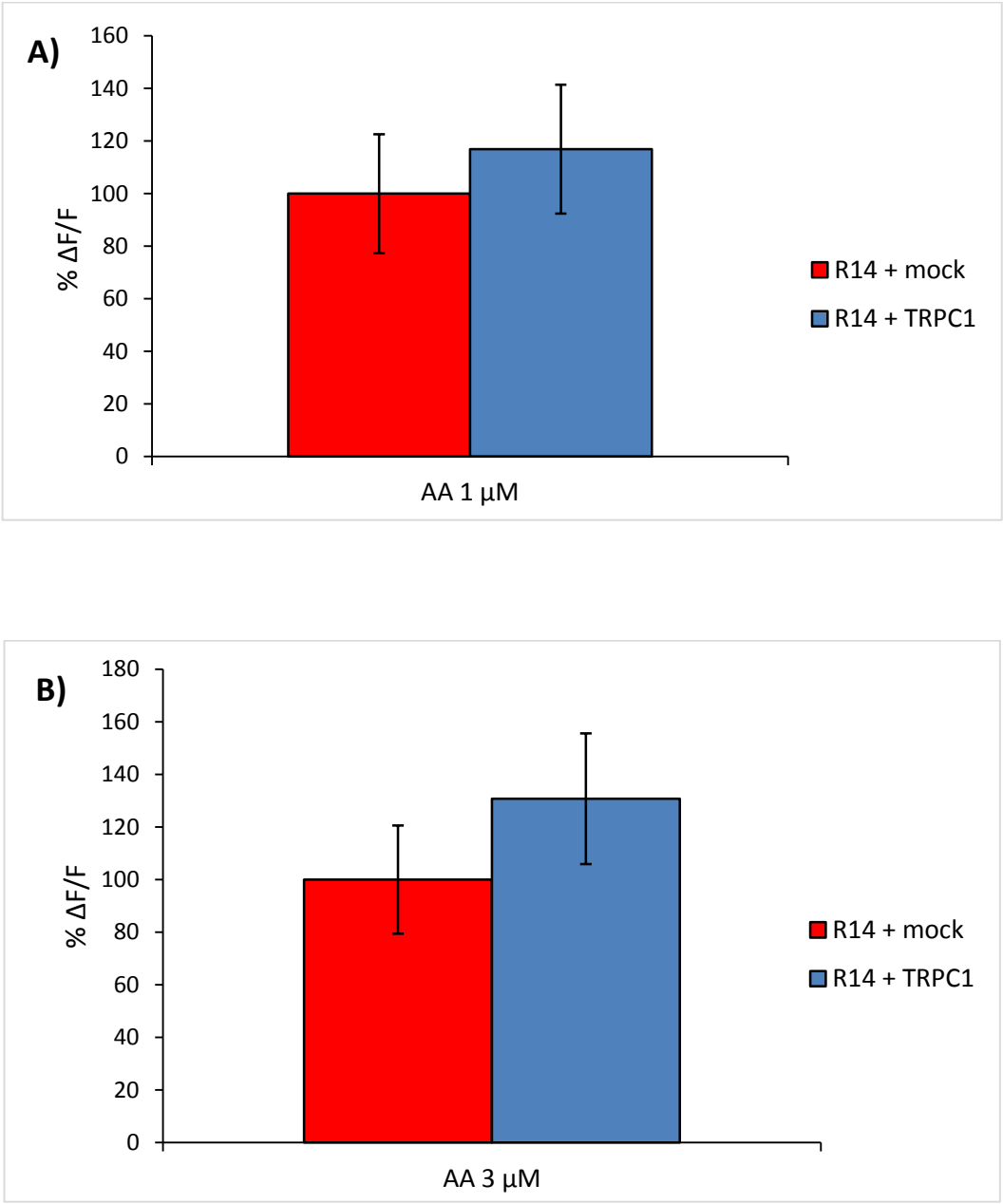

Figure 22: Histograms related to cells transfected with TAS2R14 and mock (red) and cells transfected with TAS2R14 and TRPC1 (blue), both stimulated by 1 µM (A) and 3 µM (B) aristolochic acid (indicated as AA) and corresponding standard deviation between at least three independent experiments. Y-axis: relative fluorescence intensity expressed as percent. The p-values are 0.045 and 0.007, respectively, resulting statistically significative (p-value < 0.05). In graphs signals are expressed as percentage of the signal obtained from non-TRPC1/TAS2R transfected cells.

Even cells transfected with TAS2R43 and TRPC1 have a stronger signal than cells transfected with the only TAS2R43 [Fig.23].

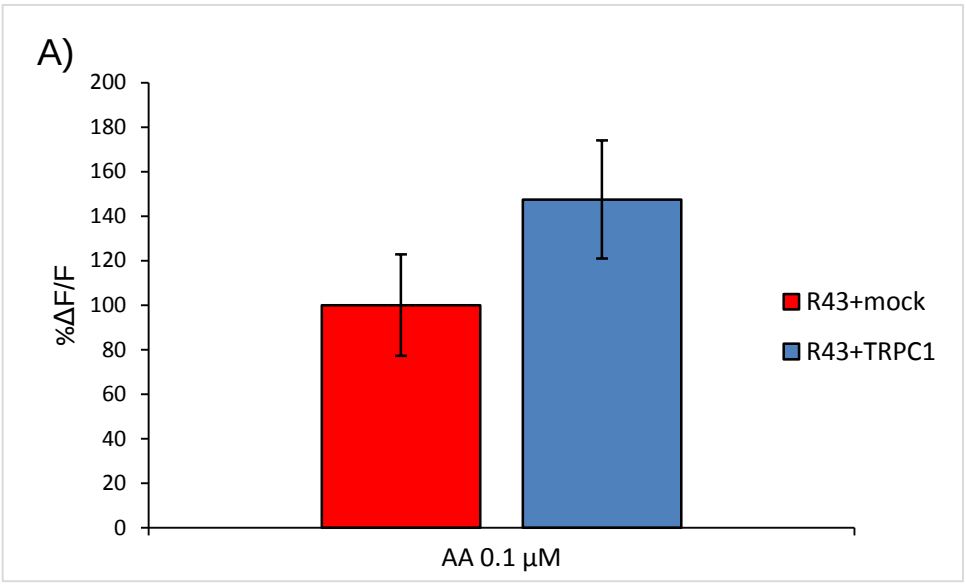

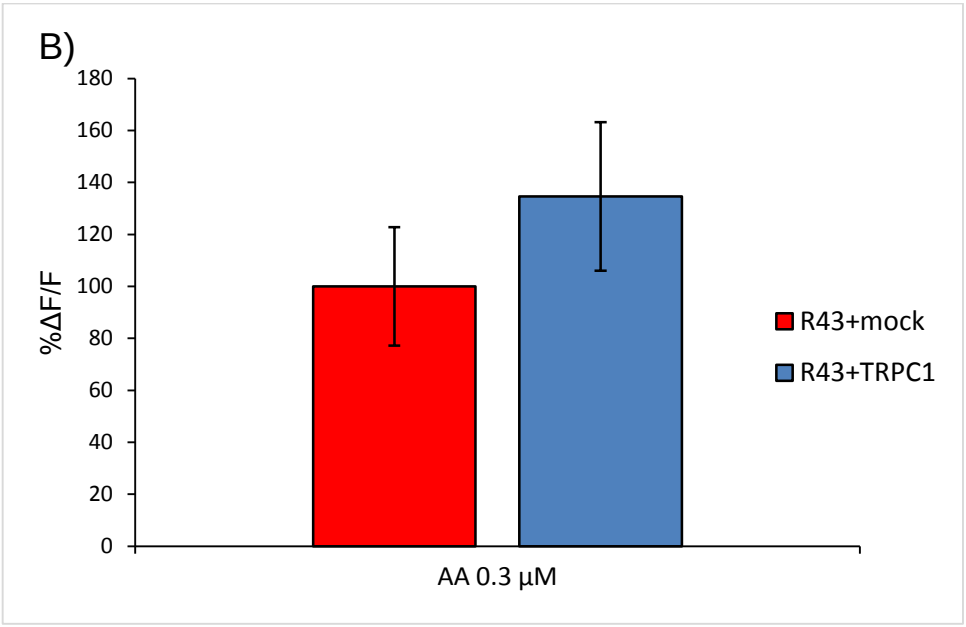

Figure 23: Histograms related to experiments with TAS2R43 transfected with TRPC1 (blue) or mock (red) and stimulated by aristolochic acid (indicated as AA) in two different concentration corresponding to 0.1 µM (A) and 0.3 µM (B) and corresponding standard deviation among at least three independent experiments. Y-axis: relative fluorescence intensity expressed as percent. Calculated p-values are in both cases 0.03 resulting statistically significative (p-value < 0.05). In graphs signals are expressed as percentage of the signal obtained from non-TRPC1/TAS2R transfected cells.

Analyzing these data through T-student test, resulting p-values were statistically significative indicating that differences between signal from test and control cells are most likely due to the presence of TRPC1 that enhances Ca^{2+} signal.

On the other hand, cells transfected with both TRPC1 and TAS2R10 showed decreased signal respect to control cells in both performed experiments [Fig.24].

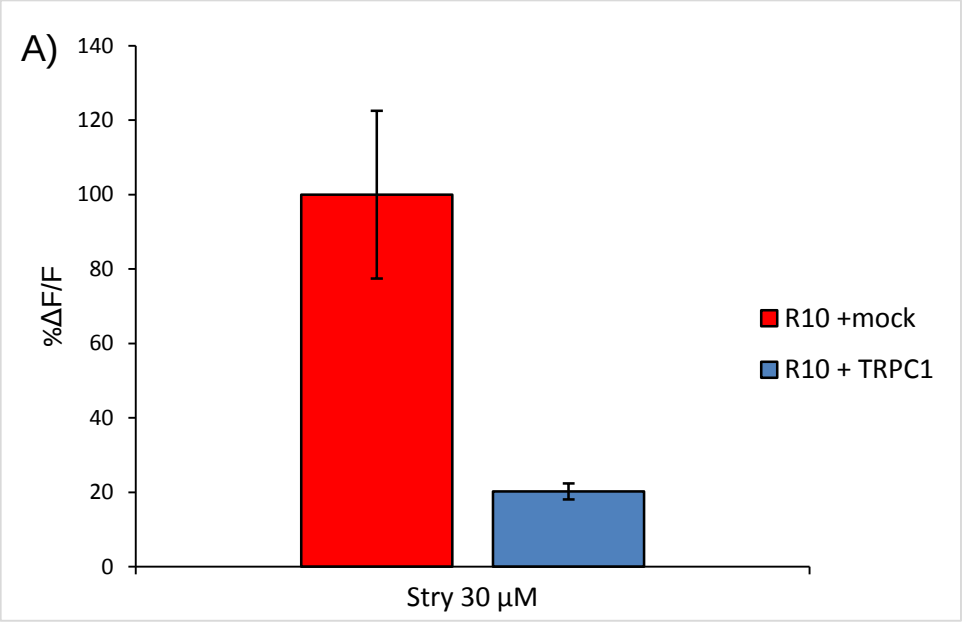

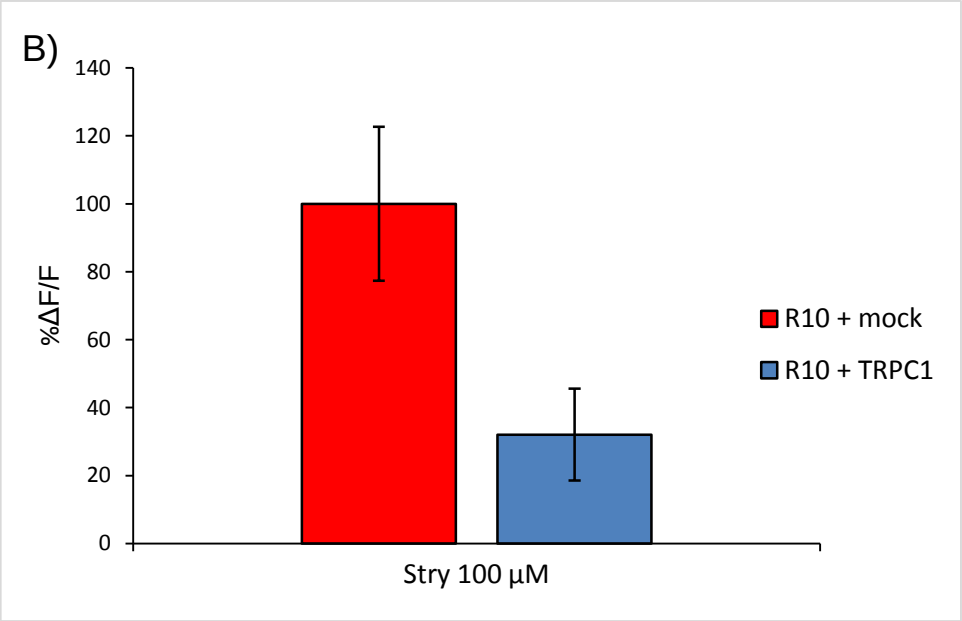

Figure 24: Histograms related to TAS2R10 transfected with TRPC1 (blue) or mock (red), stimulated by strychnine (indicated as Stry) and corresponding standard deviation between two independent experiments. Y-axis: relative fluorescence intensity expressed as percent. The used concentrations were 30 µM (A) and 100 µM (B). The p-values were 0.1 and 0.06, respectively. In graphs signals are expressed as percentage of the signal obtained from non-TRPC1/TAS2R transfected cells.

In this case the calculated p-values were 0.1 for stimulation with 30 µM solution and 0.06 with 100 µM resulting not statistical significative.

Testing TRPC1 overexpressed in HEK293T we found different results for diverse co-transfected TAS2Rs. Cells transfected with TAS2R14 or TAS2R43 and TRPC1 showed an improved signal, occurring in both experimental conditions when cells were stimulated by either concentrations. Since we obtained an increased signal, statistically confirmed by T Student test, we could affirm that co-transfection of TRPC1 could allow to overcome limitations due to receptors having low signal *per* se or could be used when a receptor is stimulated by a compound known to give a weak signal.

This conclusion yet is hampered by experiments with TAS2R10 showing a reduced signal if co-transfected with TRPC1 in both experimental condition. These results raise questions on the possibility to use TRPC1 to enhance intracellular

Ca^{2+} concentration for every taste receptor because seems to reduce TAS2R10 functionality.

Yet these data resulting opposite one another raise questions about why receptors belonging to the same family behave so differently. First hypothesis could raise from the knowledge that TAS2Rs couple with different G protein α-subunit and have also different affinity to diverse G protein βγ subunits. For instance TAS2R47 couples more efficiently with transducin, while TAS2R14 and TAS2R43 are more efficient to couple with G α_o. Moreover TAS2R47 has more affinity to $G\beta_1\gamma_1$, whereas TAS2R14 has a lower affinity for these subunits. These differences in affinity and selectivity among G protein could suggest that different TAS2Rs may activate different signal pathway (Sainz et al., 2007).

Many studies have shown that TRPC1 co-immunoprecipitated with all three IP_3 receptor types and even with the PLCβ-coupled G protein $\alpha_{q/11}$ subunit. All these elements and TRPC1 have been found in lipid raft domains, thus it is thought that they form a Ca^{2+} signal complex in those regions (Singh et al., 2001; Rosado & Sage, 2001; Lockwich et al., 2000; Singh et al., 2002).

Both the facts that TAS2Rs bind different G protein α or βγ subunits and TRPC1 would be involved in such a Ca^{2+} signal complex might interfere with the correct TAS2R10 signal cascade and thus leading to a lower signal.

It has been already reported that TAS2Rs need plasma membrane-targeting sequence to be expressed on membrane of heterologous system or auxiliary protein as receptor transporting protein (RTP) or members of the family of receptor expression enhancing proteins (REEP). But it has been shown that TAS2R10 is not higher expressed in plasma membrane when co-expressed with RTP or REEP. TAS2R10 might interacts with other not yet known chaperones, preferentially binding TRPC1 in our heterologous expression system, leading to a lower targeting of TAS2R10 to the membrane, thus to a lower signal (Chandrashekar et al., 2000; Bufe et al., 2002; Behrens et al., 2006).

Another hypothesis can be based on the observation that some substances can permeate plasma membrane and directly activate G protein (Naim et al., 1994). It is known that lipid bilayer of plasmatic membrane can be passively crossed by small molecules and non-polar molecules. Strychnine, being a plant alkaloid, is a

weak base and in water solution could be present in ionized and non-ionized forms. The latter form of strychnine could be transported by passive diffusion across the membrane and thus straight starts GPCRs signal cascade. If this were the case, TRPC1 could be activated by events after G protein activation and thus intracellular Ca^{2+} concentration would be due only to TRPC1, fitting to our results. One should also keep in mind that TRP channels can form heteromeric channels, for instance TRPC1 can bind TRPC3 (Lintschinger et al., 2000; Storch et al., 2012), TRPC4 (Hofmann et al., 2002) and TRPC5 (Hofmann et al., 2002; Strubing et al., 2001). In particular it is known that HEK293 cells already express both TRPC1 and TRPC3, hence it is possible that in our heterologous expression system the overexpressed TRPC1 interacts with the native TRPC3 forming a heterotetramer maybe not functional in co-expression with TAS2R10 (Wu et al.,2000).

More over all these events could occur all together in our expression system, leading to our unexpected result for TAS2R10.

Another aspect to consider is that GPCRs control nearly all events of eukaryotic cells physiology, thus other partners still unknown could be involved, as well as for PLCβ2 signal cascade. For instance, both roles of DAG and α-gustducin are not yet well understood.

To validate TRPC1 as a tool to improve $[Ca^{2+}]_i$ more experiments are needed. First of all, for instance, TAS2R10 should be tested with all its activators to verify if every tastant leads to a reduced signal, this could point out whether it is the receptor that behaves differently to the other TAS2Rs tested or it is rather strychnine responsible of lower signal.

More TAS2Rs should be tested in co-expression with TRPC1 trying to understand if it could be a universal tool for taste transduction model or if it works only for some receptors, whereas the others behave as TAS2R10. In the latter case it should be investigated why TAS2Rs behave differently, maybe checking implication of different G protein α-subunit, or the interaction between TRPC1 and G protein in our heterologous expression system.

Once TRPC1 will be confirmed as reliable tool leading to improved Ca^{2+} read out it could be desirable to create a cell line stably expressing TRPC1 in order to reduce

expression differences due to transient transfection. This procedure, even if performed trying to minimize every event causing fluctuations in expression level, implies differences among wells and among experiments that could impair the analysis. Furthermore differences incurring between experiments raise the necessity of a big number of tests trying to reduce the weight of experimental error on final results. Indeed our results were obtained from cells exclusively transiently transfected, thus we expect more improved signals once a cell line stably over-expressing TRPC1 will be established.

Stably expression of TRPC1 could also allow deeper investigations. For instance, it is known that TRPC1 can heteromerize with other TRP channel, thus could be possible to test co-expression of TRPC1 and TRPC4 to verify if the heteromeric channel is more functional than homomeric channel (Hofmann et al., 2002). This because several studies on TRPC1 brought to different results: Zitt et al. have found that heterologous expression gave a functional channel, whereas other studies did not detected any differences in cells over-expressing TRPC1 but found higher signal in cells co-transfected with TRPC1 and TRPC4 (reviewed in Beech et al., 2003).

If TRPC1 will be confirmed functional in our taste transduction model deeper analysis of bitter taste receptors will be possible.

4. CONCLUSIONS

The aim of the project were to find a useful tool to improve Ca^{2+} signal in the currently available model of bitter taste transduction. This necessity raised from limitations due to weak signal of some receptors in our system or low signal of a given TAS2R against a given substance (Meyerhof et al., 2010). Studies of Ca^{2+} Imaging take advantage of Ca^{2+} entry through dedicated channels and of Ca^{2+} release from internal stores. Thus, the obvious consequence was to research a channel improving intracellular Ca^{2+} concentration. It is known that taste transduction leads to empty of Ca^{2+} ER stores and it is also known that some channels are activated by this event (Roper, 2007; Parekh & Penner, 1997). Some TRP channels have been demonstrated to be activated by store depletion (reviewed in Venkatachalam & Montell, 2007). The first isolated, cloned and functionally expressed TRP channel was TRPC1 (Wes et al., 1995; Zhu et al., 1995; Zitt et al., 1996). This channel has been demonstrated being a store-operated channel and it has also demonstrated being permeable to Ca^{2+} when activated (Zitt et al., 1996). These features matched with what we were looking for. Thus we cloned TRPC1 from a sample of mRNA extract of fetal human brain and it has been functionally expressed in our taste model. The purpose was to verify if Ca^{2+} released from ER stores in consequence of TAS2R activation was able to activate TRPC1 causing a further Ca^{2+} entry from extracellular medium. Our results show that co-expression of TRPC1 and TAS2R, after stimulation of the latter by a specific tastant, leads to an improved Ca^{2+} signal at least in two cases of three tested. Thus, TRPC1 is apparently a useful tool that could be used to obtain a higher signal when it is necessary.

The possibility to improve Ca^{2+} read out will allow further analysis on TAS2Rs, maybe carrying to deorphanization of those receptors whose activators are not yet known or to discover new activators for already deorphanized TAS2Rs, widening the receptors' receptive ranges.

Moreover the response of different haplotypes could be further investigated maybe turning out that one so far thought non taster haplotype is slightly responsive instead.

Even more this system could also be used in studies about communication between taste cells and nervous system that is still poorly understood.

It might also be possible to create a mice strain over-expressing TRPC1 in taste cells and to observe whether the higher Ca^{2+} concentration after taste stimulation affects the animals' behavior. For instance if a slightly bitter substance in wild type mice could reverse in a strong aversive tastant thanks to TRPC1 over-expression, teaching more about cells communication between taste buds and nervous system and about coding of gustatory information.

If this technique will be confirmed efficient could bring important benefits not only in bitter taste studies but also with sweet and umami receptors' research, being these GPCRs too.

Another interesting application of TRPC1 over-expression could be in the study of TAS2Rs found in extra-gustatory tissues as gastrointestinal epithelium and airways. In the latter case it has been found that activation of TAS2Rs in ciliated epithelial cells increases frequency of ciliary beating (Shah et al., 2009). But TAS2Rs have been found also in airway smooth muscle cells where, when activated, lead to relaxation of smooth muscle due to activation of a BK channel. Thus, the authors suggested that inhalation of bitter compounds could be used to treat airway diseases (Deshpande et al., 2010). The problem in this case could be the bitter taste and the probable consequent adverse reaction against the medicine. Over-expression of TRPC1 could allow to find tolerable bitter compounds, which elicit a low Ca^{2+} signal but strong enough to cause muscle relaxation.

In the end improving of Ca^{2+} signal could help not only studies in taste field but also the other cases where TAS2Rs seem to have a role, leading to find out if they are involved in pathologies or if it is possible to use these receptors as a therapeutic target.

5. REFERENCES

Adler E., Hoon M.A., Mueller K.L., Chandrashekar J., Ryba N.J., Zuker C.S. 2000. A novel family of mammalian taste receptors. *Cell.* 100: 693–702.

Bartel D.L., Sullivan S.L., Lavoie E.G., Sevigny J., Finger T.E. 2006 Nucleoside triphosphate diphosphohydrolase-2 is the ecto-ATPase of type I cells in taste buds. *J. Comp. Neurol*. 497: 1–12.

Beech D.J., Xu S.Z., McHugh D., Flemming R. 2003. TRPC1 store-operated cationic channel subunit. *Cell Calcium.* 33: 433–440.

Behrens M., Bartelt J., Reichling C., Winnig M., Kuhn C., Meyerhof W. 2006. Members of RTP and REEP gene families influence functional bitter taste receptor expression. *J. Biol. Chem.* 281(29):20650-9.

Behrens M., Foertser S., Staehler F., Raguse J.D., Meyerhof W. 2007. Gustatory expression pattern of the human TAS2R bitter receptor gene family reveals a heterogeneous population of bitter responsive taste receptor cells. *J. Neurosci.* 27:12630-12640.

Born S., Levit A., Liv M.Y., Meyerhof W., Behrens M. 2013. The human bitter taste receptor TAS2R10 is tailored to accommodate numerous diverse ligands. *J. Neurosci.* 33(1):201–213.

Breslin P.A. and Spector A.C. 2008 Mammalian taste perception. *Curr. Biol.* 18(4): R148-55.

Breslin P.A. and L. Huang. 2006. Human taste: peripheral anatomy, taste transduction and coding. *Adv. Otorhinolaryngol*. 63:152–190.

Brockhoff A., Behrens M., Masha Y. N., Meyerhof W. 2010. Structure requirements of bitter taste receptor activation. *PNAS*. 107: 11110–11115

Bufe B., Hofmann T., Krautwurst D., Raguse J.D., Meyerhof W. 2002. The human TAS2R16 receptor mediates bitter taste in response to beta-glucopyranosides. *Nat Genet*. 32: 397-401

Chandrashekar J., Mueller K.L., Hoon M.A., Adler E., Feng L., Guo L., Zuker C.S., and Ryba N.J. 2000. T2Rs function as bitter taste receptors. Cell. 100:703–711.

Chandrashekar J., Hoon M.A., Ryba N.J., Zuker C.S. 2006. The receptors and cells for mammalian taste. *Nature*. 16: 444(7117):288-94.

Chandrashekar J., Kuhn C., Oka Y., Yarmolinsky D.A., Hummler E., Ryba N.J., Zuker C.S. 2010. The cells and peripheral representation of sodium taste in mice. *Nature*. 464:297–301

Chaudari N. and Roper S.D. 2010. The cell biology of taste. *JCB* 190: 285-296

Chen Y., Sun X., Herness S. 1996. Characteristic of action potentials and their underlying outward currents in rat taste receptor cells. *J Neurophysiol.* 75: 820-831.

Clapham D.E., Runnels L.W., Strubing C. 2001. The TRP ion channel family. *Nat Rev Neurosci.* 2:387–396.

Clapham D.E. 2003. TRP channels as cellular sensors. *Nature.* 426:517–524.

Clapp T.R., Stone L.M., Margolskee R.F., Kinnamon S.C. 2001 Immunocytochemical evidence for co-expression of Type III IP3 receptor with signaling components of bitter taste transduction. *BMC Neurosci*. 2:6

Clapp, T.R., R. Yang, C.L. Stoick, S.C. Kinnamon, and J.C. Kinnamon. 2004. Morphologic characterization of rat taste receptor cells that express components of the phospholipase C signaling pathway. *J. Comp. Neurol.* 468:311–321.

Damak S., Rong M., Yasumatsu K., Kokrashvili Z., Varadarajan V., Zou S., Jiang P., Ninomiya Y., Margolskee R.F. 2003. Detection of sweet and umami taste in the absence of taste receptor T1r3. *Science*. 301:850–853.

Dando R. and Roper S.D. 2009. Cell-to-cell communication in intact taste buds through ATP signalling from Pannexin 1 gap junction hemichannels. *J. Physiol*. 587:5899–5906

DeBroe M.E. 2012. Chinese herbs nephropathy and Balkan endemic nephropathy: toward a single entity, aristolochic acid nephropathy. *Kidney Int*. 81 (6): 513–5.

DeFazio R.A., Dvoryanchikov G., Maruyama Y., Kim J.W., Pereira E., Roper S.D., Chaudhari N. 2006. Separate populations of receptor cells and presynaptic cells in mouse taste buds. *J. Neurosci*. 26:3971–3980.

Deshpande D.A., Wang W.C., McIlmoyle E.L., Robinett K.S., Schillinger R.M., An S.S., Sham J.S., Liggett S.B. 2010. Bitter taste receptors on airway smooth muscle bronchodilate by localized calcium signaling and reverse obstruction. *Nat Med*; 16:1299–1304.

Drewnowski A. and Gomez-Carneros C. 2000. Bitter taste, phytonutrients, and the consumer: a review. *Am. J. Clin. Nutr*. 72:1424–35.

Dvoryanchikov G., Sinclair M.S., Perea-Martinez I., Wang T., Chaudhari N. 2009. Inward rectifier channel, ROMK, is localized to the apical tips of glial-like cells in mouse taste buds. *J. Comp. Neurol.* 517 spc1.

Farbman, A.I. 1965. Fine structure of the taste bud. *J. Ultrastruct. Res*. 12:328–350.

Finger T.E., Danilova V., Barrows J., Bartel D.L., Vigers A.J., Stone L., Hellekant G., Kinnamon S.C. 2005. ATP signaling is crucial for communication from taste buds to gustatory nerves. *Science*. 310:1495–1499.

Gudermann T., Hofmann T., Mederos y Schnitzler M., Dietrich A. 2004. Activation, subunit composition and physiological relevance of DAG-sensitive TRPC proteins. *Novartis Found Symp*. 258:103–118. Discussion 118–122, 155–109, 263–106.

Heck G.L., Mierson S., DeSimone J.A. 1984. Salt taste transduction occurs through an amiloride-sensitive sodium transport pathway. *Science*. 223:403–405.

Hofmann T., Chubanov V., Gudermann T., Montell C. 2003. TRPM5 is a voltage-modulated and Ca^{2+}-activated monovalent selective cation channel. *Curr Biol*. 13:1153–1158.

Hofmann T., Schaefer M., Schultz G., Gudermann T. 2002. Subunit composition of mammalian transient receptor potential channels in living cells. *Proc. Natl. Acad. Sci. USA.* 99:7461–7466.

Huang Y.J., Maruyama Y, Dvoryanchikov G., Pereira E., Chaudari N., Roper S.D. 2007. The role of pannexin-1 hemichannels in ATP release and cell-cell communication in mouse taste buds. *Proc. Natl. Acad. Sci. USA* 104:6436-6441

Huang Y.A., Maruyama Y., Stimac R., Roper S.D. 2008. Presynaptic (Type III) cells in mouse taste buds sense sour (acid) taste. *Journal of Physiology*. 586:2903–12.

Huang Y.A., Pereira E., Roper S.D. 2011 Acid stimulation (sour taste) elicits GABA and serotonin release from mouse taste cells. *PLoS ONE*. 6:e25471

Huang, L., Shanker Y.G., Dubauskaite J., Zheng J.Z., Yan W., Rosenzweig S., Spielman A.I., Max M., Margolskee R.F. 1999. Gγ3 co-localizes with gustducin in taste receptor cells and mediates IP_3 responses to bitter denatonium. *Nat. Neurosci*. 2:1055–1062.

Jiang P., Ji Q., Liu Z., Snyder L.A., Benard L.M, Margolskee R.F., Max M.. 2004. The cysteine-rich region of T1R3 determines responses to intensely sweet proteins. *J. Biol. Chem*. 279:45068–45075.

Kim S.J., Kim Y.S., Yuan J.P., Petralia R.S., Worley P.F., Linden D.J. 2003. Activation of the TRPC1 cation channel by metabotropic glutamate receptor mGluR1. *Nature.* 426:285–91

Kim U., Wooding S., Ricci D., Jorde L.B., Drayna D. 2005. Worldwide haplotype diversity and coding sequence variation at human bitter taste receptor loci. *Hum. Mutat.* 26:199.

Kinnamon S.C. and Finger T.E. 2013. A taste for ATP: neurotransmission in taste buds. *Front Cell Neurosci.* 7: 264.

Kuhn C., Bufe B., Winnig M., Hofmann T., Frank O., Behrens M., Lewtschenko T., Slack J.P., Ward C.D., Meyerhof W. 2004. Bitter taste receptors for saccharin and acesulfame K. *J Neurosci.* 24(45):10260-5.

Li X., Staszewski L., Xu H., Durick K., Zoller M., Adler E. 2002. Human receptors for sweet and umami taste. *Proc. Natl. Acad. Sci. USA*. 99:4692–4696.

Lintschinger B., Balzer-Geldsetzer M., Baskaran T., Graier W.F., Romanin C., Zhu M.X., Groschner K. 2000. Coassembly of TRP1 and TRP3 proteins generates diacylglycerol- and Ca^{2+}-sensitive cation channels. *J. Biol. Chem*. 275: 27799–27805.

Liu X, Bandyopadhyay B.C., Singh B.B., Groschner K., Ambudkar I.S. 2005 Molecular analysis of a store operated and 2-acetyl-sn-glycerol-sensitive non-selective cation channel. Heteromeric assembly of TRPC1-TRPC3. *J Biol Chem*. 280:21600–21606.

Liu X., Singh B.B., Ambudkar I.S. 2003. TRPC1 is required for functional store-operated Ca^{2+} channels. Role of acidic amino acid residues in the S5–S6 region. *J. Biol. Chem.* 278(13):11337–11343.

Lockwich T.P., Liu X., Singh B.B., Jadlowiec J., Weiland S., Ambudkar I.S. 2000. Assembly of Trp1 in a signaling complex associated with caveolin-scaffolding lipid raft domains. *J. Biol. Chem.* 275, 11934–11942.

Locovei S., Wang J., Dahl G. 2006. Activation of pannexin 1 channels by ATP through P2Y receptors and by cytoplasmic calcium. *FEBS Lett*. 580:239–244.

Lucas P., Ukhanov K., Leinders-Zufall T., Zufall F. 2003. A diacylglycerol-gated cation channel in vomeronasal neuron dendrites is impaired in TRPC2 mutant mice: mechanism of pheromone transduction. *Neuron.* 40(3):551-61.

Lyall V., Alam R.I., Phan D.Q., Ereso G.L., Phan T.H., Malik S.A., Montrose M.H., Chu S., Heck G.L., Feldman G.M., DeSimone J.A.. 2001. Decrease in rat taste receptor cell intracellular pH is the proximate stimulus in sour taste transduction. *Am. J. Physiol. Cell Physiol*. 281:C1005–C1013

Martin B., Maudsley S., White C.M., Egan J.M. 2009. Hormones in the naso-oropharynx: Endocrine modulation of taste and smell. *Trends Endocrinol Metab*. 20(4): 163–170.

Mast T.G., Brann J.H., Fadool D.A. 2010. The TRPC2 channel forms protein-protein interactions with Homer and RTP in the rat vomeronasal organ. *BMC Neurosci.* 11:61.

Max M., Shanker Y.G., Huang L., Rong M., Liu Z., Campagne F., Weinstein H., Damak S., Margolskee R.F. 2001. Tas1r3, encoding a new candidate taste receptor, is allelic to the sweet responsiveness locus Sac. *Nat. Genet*. 28:58–63.

McLaughlin S.K., McKinnon P.J., Margolskee R.F. 1992. Gustducin is a taste-cell-specific G protein closely related to the transducins. *Nature*. 18: 357 (6379):563-9.

Mennella J.A., Spector S.C, Reed D.R., Coldwell S.E. 2013. The bad taste of medicines: overview of basic research on bitter taste. *Clin Ther*. 35(8): 1225–1246.

Meyerhof W. 2005. Elucidation of mammalian bitter taste. *Rev. Physiol. Biochem. Pharmacol.* 154: 37.

Meyerhof W., Batram C., Kuhn C., Brockhoff A., Chudoba E., Bufe B., Appendino G., Behrens M. 2010. The molecular receptive ranges of human TAS2R bitter taste receptors. *Chem. Senses*. 35:157–170.

Michling S., Damak S., Le Coutre J. 2007. Claudin-based permeability barriers in taste buds. *J. Comp. Neurol*. 502:1003–1011.

Minke B. 2001 The TRP channel and phospholipase C-mediated signaling. *Cell Mol. Neurobiol.* 21(6):629-43.

Miyoshi M.A., Abe K., Emori Y. 2001. IP (3) receptor type 3 and PLCβ2 are co-expressed with taste receptors T1R and T2R in rat taste bud cells. *Chem Senses*. 26(3):259-65.

Murray R.G. 1993. Cellular relations in mouse circumvallate taste buds. *Microsc. Res. Tech*. 26:209–224.

Naim M., Seifert R., Nurnberg B., Grunbaum L., Schultz G. 1994. Some taste substances are direct activators of G-proteins. *Biochem J*. 297:451–454.

Nelson G., Chandrashekar J., Hoon M.A., Feng L., Zhao G., Ryba N.J., Zuker C.S. 2002. An amino-acid taste receptor. *Nature*. 416:199–202.

Nelson G., Hoon M.A., Chandrashekar J., Zhang Y., Ryba N.J., Zuker C.S. 2001. Mammalian sweet taste receptors. *Cell*. 106:381–390.

Ong E.C., Nesin V., Long C.L., Bai C.X., Guz J.L., Ivanov I.P., Abramowitz J., Birnbaumer L., Humphrey M.B., and Tsiokas L. 2013. A TRPC1 protein-dependent pathway regulates osteoclast formation and function. *J Biol Chem.* 288(31): 22219–22232.

Parekh A.B., Penner R. 1997 Store depletion and calcium influx. *Physiological Reviews*. 77(4):901–930.

Perez C.A., Huang L., Rong M., Kozak J.A., Preuss A.K., Zhang H., Max M., Margolskee R.F. 2002. A transient receptor potential channel expressed in taste receptor cells. *Nat Neurosci*. 5:1169–1176.

Prawitt D., Monteilh-Zoller M.K., Brixel L., Spangenberg C., Zabel B., Fleig A., Penner R. 2003. TRPM5 is a transient Ca^{2+}-activated cation channel responding to rapid changes in [Ca^{2+}] i. *Proc Natl Acad Sci U S A*. 100(25):15166-71.

Pronin A.N., Xu H., Tang H., Zhang L., Li. Q., Li X. 2007. Specific alleles of bitter receptor genes influence human sensitivity to the bitterness of aloin and saccharin. *Curr. Biol.* 17, 1403.

Pumplin D.W., Yu C., Smith D.V. 1997. Light and dark cells of rat vallatae taste buds are morphologically distinct cell types. *J. Comp. Neurol.* 378:389–410.

Reichling C., Meyerhof W., Behrens M. 2008. Functions of human bitter taste receptors depend on N-glycosylation. *J Neurochem.* 106(3):1138-48

Romanov R.A., Bystrova M.F., Rogachevskaja O.A., Sadovnikov V.B., Shestopalov V.I., Kolesnikov S.S. 2012. Dispensable ATP permeability of Pannexin 1 channels in a heterologous system and in mammalian taste cells. *J Cell Sci*. 125(Pt 22):5514-23

Romanov R.A., Rogachevskaja O.A., Bystrova M.F., Jiang P., Margolskee R.F., Kolesnikov S.S. 2007. Afferent neurotransmission mediated by hemichannels in mammalian taste cells. *EMBO J*. 26:657–667

Roper S.D. 2007. Signal transduction and information processing in mammalian taste buds. *Pflugers Arch*. 454(5):759-76.

Rosado J.A., Sage S.O. 2001. Activation of store-mediated calcium entry by secretion-like coupling between the inositol 1, 4, 5-trisphosphate receptor type II and human transient receptor potential (hTrp1) channels in human platelets. *Biochem. J.* 356, 191–198.

Rössler P., Kroner C., Freitag J., Noè J., Breer H. 1998. Identification of a phospholipase Cβ subtype in rat taste cells*. Eur. J. Cell Biol*. 77:253–261.

Sainz E., Cavenagh M.M., Gutierrez J., Battey J.F., Northup K.J., Sullivan S.L. 2007. Functional characterization of human bitter taste receptors. *Biochem. J.* 403:537–543.

Schaefer M. 2005. Homo- and heteromeric assembly of TRP channel subunits. *Pflugers Arch.* 451:35–42.

Shah A.S., Ben-Shahar Y., Moninger T.O., Kline J.N., Welsh M.J. 2009. Motile cilia of human airway epithelia are chemosensory. *Science*; 325:1131–1134.

Shi P., Zhang J. 2006. Contrasting modes of evolution between vertebrate sweet/umami receptor genes and bitter receptor genes. *Mol. Biol. Evol.* 23:292–300.

Singh B.B, Zheng C., Liu X. 2001 Trp1-dependent enhancement of salivary gland fluid secretion: role of store-operated calcium entry. *FASEB J.* 15:1652–1654.

Singh B.B., Liu X., Tang J., Zhu M.X., Ambudkar I.S. 2002. Calmodulin regulates Ca2+-dependent feedback inhibition of store-operated Ca^{2+} influx by interaction with a site in the C terminus of TRPC1. *Mol. Cell.* 9: 739–750.

Storch U.; Mederos y Schnitzler M.; Gudermann T. 2012. G protein-mediated stretch reception. *Am. J. Physiol Heart Circ. Physiol.* 302: H1241–H1249.

Strubing C., Krapivinsky G., Krapivinsky L., Clapham D.E. 2001 TRPC1 and TRPC5 form a novel cation channel in mammalian brain. *Neuron.* 29:645–655.

Tomchik S.M., Berg S., Kim J.W., Chaudhari N., Roper S.D. 2007. Breadth of tuning and taste coding in mammalian taste buds. *J. Neurosci*. 27:10840–10848.

Ueda T., Ugawa S., Yamamura H., Imaizumi Y., Shimada S. 2003. Functional interaction between T2R taste receptors and G-protein α subunits expressed in taste receptor cells. *J Neurosci.* 23(19):7376-80.

Vandenbeuch A., Clapp T.R., Kinnamon S.C. 2008 Amiloride-sensitive channels in type I fungiform taste cells in mouse. *BMC Neuroscience:* 9:1.

Vandenbeuch A. and Kinnamon S.C. 2009. Why do taste cells generate action potentials? *J. Biol*. 8:42.

Venkatachalam K. and Montell C. 2007. TRP channels*. Annu. Rev. Biochem*. 76: 387-417.

Wes P.D., Chevesich J., Jeromin A., Rosenberg C., Stetten G., Montell C. 1995. TRPC1, a human homolog of a Drosophila store-operated channel*. Proc. Natl. Acad. Sci. USA* 92, 9652–9656.

Wu X., Babnigg G., Villereal M.L. 2000. Functional significance of human trp1 and trp3 in store-operated Ca^{2+} entry in HEK-293 cells. *Am. J. Physiol. Cell Physiol*. 278:C526–C536.

Xu H., Staszewski L., Tang H., Adler E., Zoller M., Li X. 2004. Different functional roles of T1R subunits in the heteromeric taste receptors. *Proc. Natl. Acad. Sci. USA*. 101:14258–14263.

Yang R., Crowley H.H., Rock M.E., Kinnamon J.C. 2000. Taste cells with synapses in rat circumvallate papillae display SNAP-25-like immunoreactivity. *J. Comp. Neurol*. 424:205–215.

Yarmolinsky D.A., Zuker C.S., Ryba N.J. 2009. Common sense about taste: from mammals to insects. *Cell*. 139:234–44.

Yee C.L., Yang R., Böttger B., Finger T.E, Kinnamon J.C. 2001. “Type III” cells of rat taste buds: immunohistochemical and ultrastructural studies of neuron-specific enolase, protein gene product 9.5, and serotonin. *J. Comp. Neurol.* 440:97–108.

Yoshida R., Miyauchi A., Yasuo T., Jyotaki M., Murata Y., Yasumatsu K., Shigemura N., Yanagawa Y., Obata, Ueno H., et al. 2009a. Discrimination of taste qualities among mouse fungiform taste bud cells. *J. Physiol*. 587:4425–4439.

Zhang P., Yang C., Delay R.J. 2010 Odors activate dual pathways, a TRPC2 and an AA-dependent pathway, in mouse vomeronasal neurons. *Am J Physiol Cell* Physiol. 298(5):C1253-64.

Zhang Z., Zhao Z., Margolskee R.F., Liman E.R. 2007 The transduction channel TRPM5 is gated by intracellular calcium in taste cells. *J Neurosci*. 27:5777–5786.

Zhu X., Chu P. B., Peyton, M., Birnbaumer, L. 1995. Molecular cloning of a widely expressed human homologue for the Drosophila trp gene. *FEBS Lett*. 373:193-198.

Zitt C., Zobel A., Obukhov A.G., Harteneck C., Kalkbrenner F., Lückhoff A., Schultz G. 1996. Cloning and functional expression of a human Ca^{2+}-permeable cation channel activated by calcium store depletion. *Neuron*. 16: 1189-1196.

RINGRAZIAMENTI

Vorrei iniziare ringraziando la mia famiglia per tutto quello che hanno fatto durante i miei anni universitari, senza di loro non sarei arrivata fin qui.

Non meno importante è stato il supporto e l'amore incondizionato di Federico al quale ho chiesto molto.

Preziosissimo è stato l'aiuto di Alessandro, sia in laboratorio e durante la stesura di questa tesi sia per la sua amicizia. Senza di lui non sarebbe stata la stessa esperienza.
Ringrazio anche il Prof. Dal Monte per avermi offerto la possibilità di questa esperienza, la quale mi ha insegnato molto.

Infine ringrazio chiunque ci sia stato e chi no, sono convinta che ogni situazione vissuta insegni qualcosa e quindi tutto è prezioso.

"…that's the end and that's the start…"